

NASA/TM—2001-210984



Analysis of Fade Detection and Compensation Experimental Results in a Ka-Band Satellite System

Sandra Johnson
Glenn Research Center, Cleveland, Ohio

July 2001

The NASA STI Program Office . . . in Profile

Since its founding, NASA has been dedicated to the advancement of aeronautics and space science. The NASA Scientific and Technical Information (STI) Program Office plays a key part in helping NASA maintain this important role.

The NASA STI Program Office is operated by Langley Research Center, the Lead Center for NASA's scientific and technical information. The NASA STI Program Office provides access to the NASA STI Database, the largest collection of aeronautical and space science STI in the world. The Program Office is also NASA's institutional mechanism for disseminating the results of its research and development activities. These results are published by NASA in the NASA STI Report Series, which includes the following report types:

- **TECHNICAL PUBLICATION.** Reports of completed research or a major significant phase of research that present the results of NASA programs and include extensive data or theoretical analysis. Includes compilations of significant scientific and technical data and information deemed to be of continuing reference value. NASA's counterpart of peer-reviewed formal professional papers but has less stringent limitations on manuscript length and extent of graphic presentations.
- **TECHNICAL MEMORANDUM.** Scientific and technical findings that are preliminary or of specialized interest, e.g., quick release reports, working papers, and bibliographies that contain minimal annotation. Does not contain extensive analysis.
- **CONTRACTOR REPORT.** Scientific and technical findings by NASA-sponsored contractors and grantees.

- **CONFERENCE PUBLICATION.** Collected papers from scientific and technical conferences, symposia, seminars, or other meetings sponsored or cosponsored by NASA.
- **SPECIAL PUBLICATION.** Scientific, technical, or historical information from NASA programs, projects, and missions, often concerned with subjects having substantial public interest.
- **TECHNICAL TRANSLATION.** English-language translations of foreign scientific and technical material pertinent to NASA's mission.

Specialized services that complement the STI Program Office's diverse offerings include creating custom thesauri, building customized data bases, organizing and publishing research results . . . even providing videos.

For more information about the NASA STI Program Office, see the following:

- Access the NASA STI Program Home Page at <http://www.sti.nasa.gov>
- E-mail your question via the Internet to help@sti.nasa.gov
- Fax your question to the NASA Access Help Desk at 301-621-0134
- Telephone the NASA Access Help Desk at 301-621-0390
- Write to:
NASA Access Help Desk
NASA Center for Aerospace Information
7121 Standard Drive
Hanover, MD 21076

NASA/TM—2001-210984



Analysis of Fade Detection and Compensation Experimental Results in a Ka-Band Satellite System

Sandra Johnson
Glenn Research Center, Cleveland, Ohio

National Aeronautics and
Space Administration

Glenn Research Center

July 2001

Acknowledgments

I would like to acknowledge the numerous people who have assisted me in the completion of this degree. Thank you to my management at NASA Glenn Research Center for allowing me to pursue this educational opportunity, most specifically to Dr. Roberto Acosta for his technical assistance, support, and patience. I would also like to thank my advisor, Dr. Oke Ugweje, for his guidance.

Available from

NASA Center for Aerospace Information
7121 Standard Drive
Hanover, MD 21076

National Technical Information Service
5285 Port Royal Road
Springfield, VA 22100

Available electronically at <http://gltrs.grc.nasa.gov/GLTRS>

TABLE OF CONTENTS

	Page
LIST OF TABLES	vi
LIST OF FIGURES	vii
CHAPTER	
I. INTRODUCTION	1
1.1 Propagation Impairments and Compensation	1
1.2 Problem Statement	2
1.3 Scope of Research	3
1.4 Thesis Overview	4
II. SYSTEM DESCRIPTION	7
2.1 Background	7
2.2 Link Margins, Fade Detection and Compensation	9
2.3 Cumulative Distribution of Fade	10
2.4 Advanced Communication Technology Satellite	13
2.4.1 Spacecraft Description	13
2.4.2 ACTS Communication Protocol	15
2.4.3 ACTS Control Network	17
2.5 T1 VSAT Description	17
2.5.1 ACTS Fade Detection	19
2.5.2 ACTS Fade Compensation	21

	Page
2.5.3 ACTS Clear Sky Margins	23
III. COMPENSATION EXPERIMENT DESCRIPTION AND ANALYSIS	25
3.1 Hardware Connectivity	25
3.2 Sample of Post-Processed Experimental Data	27
3.2.1 Correlation of Rain Event with BER and E_b/N_0	28
3.2.2 Sample Cumulative Distribution Data	30
3.3 System Calibration	33
3.4 Compensation Experiment Data Analysis	38
3.4.1 Statistical Analysis	38
3.4.2 Time Series Analysis	42
3.5 Derived BER Time Enhancement Factor for the ACTS Algorithm	488
3.6 Summary of Compensation Experiment Results	51
IV. DERIVED TECHNIQUES FOR FUTURE SYSTEM ANALYSIS	53
4.1 Bit Error Rate Time Enhancement Factor	53
4.2 Software Model	53
4.3 Results from Software Model using APT Data	55
4.4 Experimental BER Distribution	59
V. CONCLUSION	61
5.1 Summary	61
5.2 Suggestions for Improvement	62
5.3 Suggestions for Implementation on Future Communication Systems	63
BIBLIOGRAPHY	65

	Page
APPENDICES	69
Appendix 1: Link Budget for the ACTS Compensation Experiment	70
Appendix 2: SIMULINK Model of Convolutional Coding	76
Appendix 3: MATLAB Code for Generating BER Time Enhancement Factor for ACTS Propagation Terminal Data	77
INDEX OF SYMBOLS	81

LIST OF TABLES

Table	Page
2.1: T1 VSAT Operational Features	18
2.2: ACTS T1 VSAT Theoretical Link Budget Results in Cleveland, Ohio	24
4.1 : ACTS Propagation Measurement Sites	55

LIST OF FIGURES

Figure	Page
2.1: Typical Cumulative Distribution of Fade	11
2.2: Location of Five Sites for CDF in Figure 2.1	12
2.3: The ACTS Spacecraft	14
2.4: ACTS Hopping Spot Beams	15
2.5: ACTS Downlink TDMA Frame Architecture	16
2.6: T1 VSAT Indoor Unit	18
2.7: T1 VSAT Outdoor Unit	18
2.8: Sample ONSET and CESSATION Threshold Settings	23
3.1: Hardware Configuration for BER Measurement	26
3.2: Experiment Photo of VSATs, Tipping Bucket, and Ground Station Antenna	27
3.3: Fade and Rain Rate for Sample Rain Event	29
3.4: Downlink BER for Sample Rain Event	29
3.5: Uplink BER for Sample Rain Event	30
3.6: Distribution of Fade for Sample Rain Event	31
3.7: Distribution of Downlink BER for Sample Rain Event	32
3.8: Distribution of Uplink BER for Sample Rain Event	32
3.9: Fades Results for Calibration Experiment	35
3.10: Downlink BER Results for Calibration Experiment	35

Figure	Page
3.11: Uplink BER Results for Calibration Experiment	36
3.12: Distribution of Fade for Calibration Experiment	36
3.13: Distribution of Downlink BER for Calibration Experiment	37
3.14: Distribution of Uplink BER for Calibration Experiment	37
3.15: Distribution of Fade for Compensation Experiment	40
3.16: Distribution of Downlink BER for Compensation Experiment	40
3.17: Distribution of Uplink BER for Compensation Experiment	41
3.18: Rain Rate Distribution for Cleveland, Ohio	42
3.19: E_b/N_0 for Rain Fade Event (August 8, 1999)	44
3.20: Downlink BER for Rain Fade Event (August 8, 1999)	44
3.21: Uplink BER for Rain Fade Event (August 8, 1999)	45
3.22: E_b/N_0 for Rain Fade Event (May 24, 1999)	45
3.23: Downlink BER for Rain Fade Event (May 24, 1999)	46
3.24: Uplink BER for Rain Fade Event (May 24, 1999)	46
3.25: E_b/N_0 for Rain Fade Event (September 29-30, 1999)	47
3.26: Downlink BER for Rain Fade Event (September 29-30, 1999)	47
3.27: Uplink BER for Rain Fade Event (September 29-30, 1999)	48
3.28: Distribution of Downlink BER for Compensation Experiment	49
3.29: Distribution of Uplink BER for Compensation Experiment	50
3.30: Measured BER Time Enhancement Factor	50
4.1: Location of Seven ACTS Propagation Terminals	55

Figure	Page
4.2: Distribution of Rain for Seven ACTS Propagation Terminals	56
4.3: CDF of Fade using ACTS Propagation Terminals at 20 GHz	57
4.4: Performance of Uncoded and Coded BPSK	57
4.5: BER Time Enhancement Factor using ACTS Propagation Terminals	58
4.6: Comparison of Measured and Theoretical BER Distribution	60

CHAPTER I

INTRODUCTION

1.1 Propagation Impairments and Compensation

The carrier frequencies to be implemented for a communication satellite system are a primary design parameter and are chosen based on a number of factors. A carrier frequency that is too low may not penetrate the ionosphere. A carrier frequency that is too high correlates to a wavelength so small that the properties of the wave could be degraded to the point where communication becomes impossible. These degradations to the wave produced by a very short wavelength can cause a reduction in signal amplitude (attenuation), depolarization of the radiowave, and an increase in thermal noise (radio noise) in the system. In frequency bands above 10 GHz, the wavelength is within the size range of a rain drop, causing it to be easily absorbed by the rain. This attenuation due to rain can cause major impairments in space communications [1]. Other factors contributing to rain degradation include antenna elevation angle and polarization, earth station altitude, receiver noise temperature and local meteorology.

In order for commercial systems to generate a significant amount of revenue, the amount of information per unit time must be increased from current levels. This increase in information transfer requires large bandwidths that are only available at frequencies higher than Ku-band. In addition, since most current commercial systems operating

today use the C-band (6/4 GHz) and Ku-band (14/11 GHz), very few extra spectrum slots are available in this range. This limits growth and demand for new and enhanced video and data services and represents one of the most significant reasons for new systems to operate in the Ka-band (30/20 GHz) and above.

Because of the considerable advantages of operating a satellite communication system in the higher frequency ranges, compensation techniques have been developed to overcome the impairments associated with these frequency bands. These compensation techniques improve the communication performance by enabling the transmitted signal to withstand the effects of various channel impairments, such as noise, fading, and jamming.

1.2 Problem Statement

The objective of this thesis is to perform a statistical investigation and validation of the rain fade detection and compensation algorithm in an end-to-end Ka-band satellite system. Results from this investigation are provided and analyzed and limitations in the technique are stated. An algorithm is developed to determine the impact of data compensation techniques, which can be used for future system analysis.

Determining the impact of a chosen coding and modulation scheme for an arbitrary environment is critical in determining the availability of the system for a specified bit error rate. A process is developed in this thesis that can be used to estimate the bit error rate time enhancement for an arbitrary location, modulation and coding technique. Given the fade cumulative distribution function (CDF) and bit error rate (BER) versus bit energy per noise ratio (E_b/N_0) performance curves for the coded and uncoded modulation

technique chosen, the process provides as an output the amount of additional availability which can be gained by incorporating coding into the system. This value, referred to as the BER time enhancement factor, is the additional percent of time which a coded link will maintain or exceed a given BER level over a link system that is not coded. This process is applied to a number of actual fade distributions in a range of environments to demonstrate its use. Based on these results, the benefit of coding in different environments can be observed.

Implementation issues, such as estimating the E_b/N_0 value, determining the threshold settings for which coding should adaptively be applied and removed, and the BER collection technique, are discussed and suggestions for improvement are given.

1.3 Scope of Research

The measured data used for analysis was collected at the NASA Glenn Research Center in Cleveland, Ohio from May 1999 to February 2000 using the Advanced Communication Technology Satellite. Cleveland, Ohio is located in ITU-R rain zone K (a medium rain zone). Approximately 6 station years of data was collected, which included uplink and downlink bit error rates and downlink fade data for both VSATs and rain data. The collected BER is an average BER over a two-minute period, and the theoretical BER is generally an instantaneous BER for the given E_b/N_0 . This difference introduces an error when theoretical and measured data are compared. At high E_b/N_0 values (greater than 13 dB in this experiment), no bit errors will be observed during the two-minute collection period, and the reported BER is 0. This value is arbitrarily

changed to 5×10^{-9} in the database to avoid errors when plotting the log of the BER. Because the uplink carrier frequency (29 GHz) is higher than the downlink carrier frequency (19 GHz), and the control station must remain synchronized with the uplink data, the uplink BER is the limiting factor for the VSAT to remain synchronized with the control station. For this reason, the uncoded VSAT generally loses synchronization with the control station at a E_b/N_0 of 6 dB and the coded VSAT at 1 dB. This limits the range of valid E_b/N_0 to be 6 to 13 dB for the uncoded VSAT and 1 to 13 dB for the coded VSAT.

The downlink BER from the remote test set is downloaded to the control station via a modem using the satellite link to the VSAT. When the downlink BER exceeds 10^{-4} , the uplink is so degraded that the BER modem can no longer obtain data. This causes uplink BER rates greater than 10^{-4} to not be recorded. A calibration experiment was performed which collected downlink BER through a modem connected terrestrially to provide a more accurate understanding of the relationship between E_b/N_0 and BER.

1.4 Thesis Overview

In the next chapter, a general description of the ACTS satellite network, a discussion of available methods used to detect and compensate for rain fade, and the ACTS fade detection and compensation techniques are presented. A review of previous work in the area of availability enhancement techniques and the uniqueness of the analysis conducted for this thesis is also examined. Chapter 3 presents a description of the experiment performed to study the ACTS fade detection and compensation technique.

This includes diagrams and photographs of the experiment setup along with sample data analyzed using statistical and time series data. The results from an ACTS calibration experiment are presented and analyzed as well. Chapter 4 describes the algorithm developed to calculate the BER time enhancement factor. This technique provides a model to be used to determine the increase in availability that might be realized by the addition of data coding in a given environment. Sample results using measured fade data are presented. Results derived from the analysis are also presented. Finally, Chapter 5 summarizes the main results, discusses other methods used for fade detection, and provides suggestions on how to improve the ACTS fade compensation techniques.

CHAPTER II

SYSTEM DESCRIPTION

2.1 Background

Data has been collected and analyzed using ACTS and other satellite systems with Ka-band communication capabilities or beacons, including Olympus and Italsat. Olympus was a European Space Agency satellite that was launched in 1989 and carried a payload to offer new services with its steerable spot beams operating in the Ka-band to VSAT stations with 0.8 and 1.8 m antennas. Olympus also carried beacons for propagation studies in the Ka-band. Olympus operated until 1993 when the satellite ran out of fuel [2]. Italsat is an advanced telecommunications program of the Italian Space Agency (ASI) [3]. Italsat operates in the Ka-band using digital technology. Two satellites make up the Italsat system: F1, launched in 1991; and F2, launched in 1996. The ACTS system is the only Ka-band satellite system with a fast-acting beam forming network which allows each spot beam to switch locations in less than a microsecond. Rather than having fixed beams with a separate transponder devoted to each beam location, the ACTS switching or hopping beams allow a single transponder to be shared among many beam locations. The other advancement provided by ACTS is the onboard

baseband processor which allows complete mesh interconnectivity on an individual circuit basis [4].

The experiment developed for this thesis represents the first time that two identical ground stations, one employing adaptive fade compensation techniques and one with no compensation enabled, have been placed in the same geographic area and data collected for an extended period. The effect of the adaptive compensation is analyzed and the BER time enhancement factor realized by the coding technique is developed. Using the developed characterization process, the results can be generalized for other rain regions, modulations, and coding techniques.

The ACTS Propagation Campaign was developed to provide a thorough understanding of Ka-band propagation issues, to develop models for the prediction of propagation related anomalies, and to develop tools for the mitigation of these anomalies. These objectives were achieved by making long-term measurements at seven sites located in 6 different rain zones and analyzing the collected data. This campaign relied on unique terminals developed for this project called the ACTS Propagation Terminals (APT) [7]. The APTs were receive-only terminals that used a beacon to measure the downlink quality instead of the communications channel, as was done with the T1 VSATs. Distribution functions of the fade depths developed from the campaign are used in this thesis to illustrate how the results from this thesis can be applied to different environments [8].

2.2 Link Margins, Fade Detection and Compensation

To determine a satellite system's operational capability, a link budget is performed which calculates the useful signal power and interfering noise power available at the receiver. This determines the satellite system's capability to "close the link" – or operate at the required error performance.

Because of noise and other impairments in the system, additional gain is designed into the system. This additional gain is referred to as the "margin". When the methods used to develop the margin are unchangeable, they are "fixed margins". If enough fixed margin were added to a system to compensate for major fades, the cost would be prohibitive and the additional margin would only be required a very small percentage of the time [7]. Therefore, it is advantageous to develop a satellite system with a small fixed margin and employ adaptive techniques to implement the additional margins that are required only when the required link budget exceeds the fixed margin.

In order to accurately determine the need for adaptive compensation, the level of the system's attenuation (or fade) must be measured. A commonly used method involves measuring the beacon signals at the uplink and downlink frequencies and basing the estimate on the received power levels. Another method is to use the demodulated burst signal from the satellite and determine the Signal-to-Noise Ratio (SNR) using some type of statistical measurement [8].

Many adaptive compensation techniques have been developed. These include the use of an adaptive antenna system [9], adaptive modulation schemes [7], orbital and spatial diversity [10], power control [11], and data coding techniques [12], [13], [14].

2.3 Cumulative Distribution of Fade

A common method to statistically represent the measured link data at a particular location is by using a Cumulative Distribution Function (CDF) of the fade. This representation provides a simple method to determine what percentage of the time a certain fade was exceeded at a given location. By studying this data, a system engineer can determine the amount of time that the fade would exceed the specified operating availability and how often adaptive compensation techniques are needed. The CDF for other variables, such as BER, is also an invaluable tool to understanding the operational characteristics of the system. An example of the fade CDF from five experimental locations is shown in Figure 2.1. A detailed description of the five locations and a diagram of the locations with respect to ITU rain zones is shown in Figure 2.2.

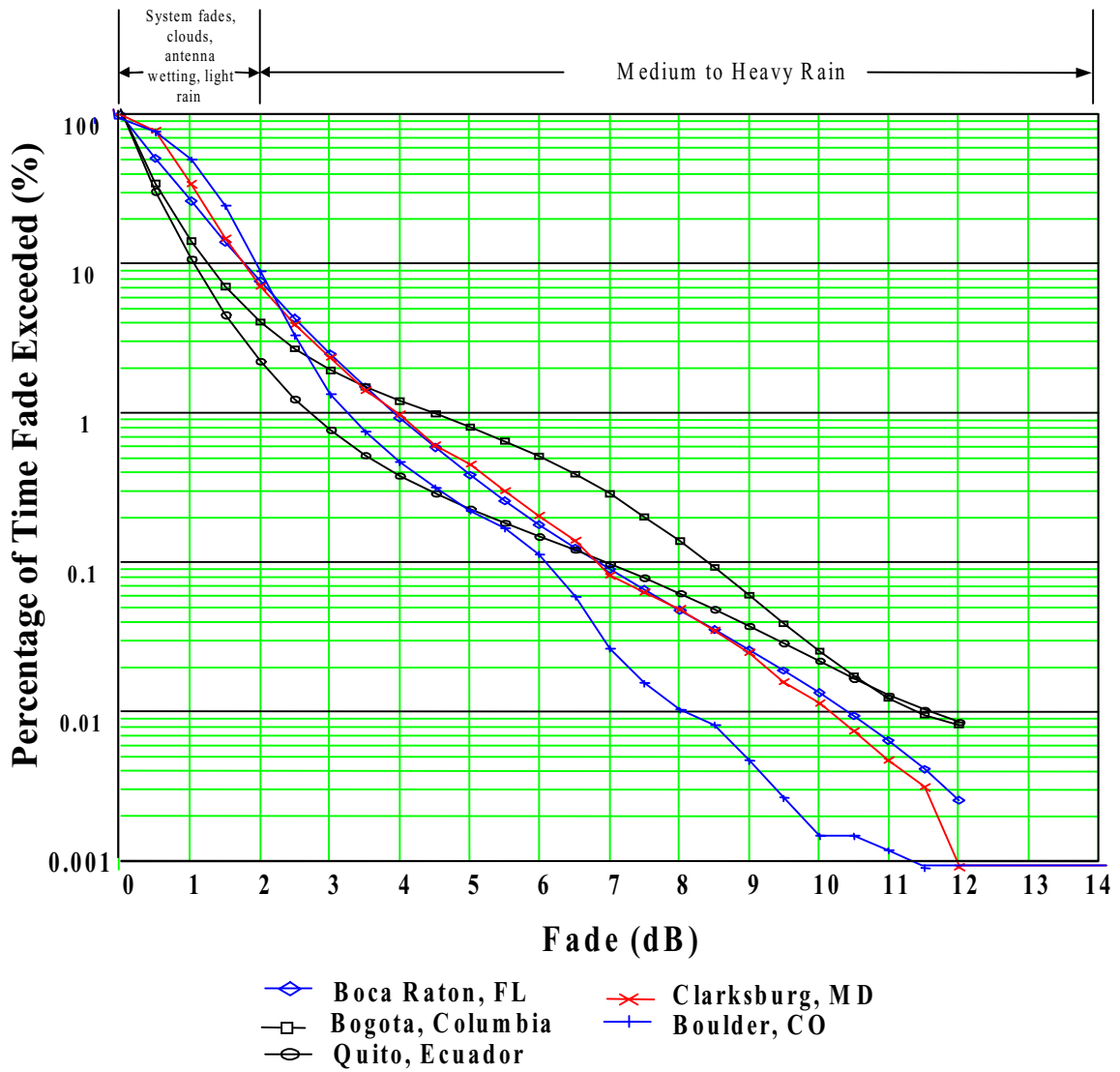


Figure 2.1: Typical Cumulative Distribution of Fade.

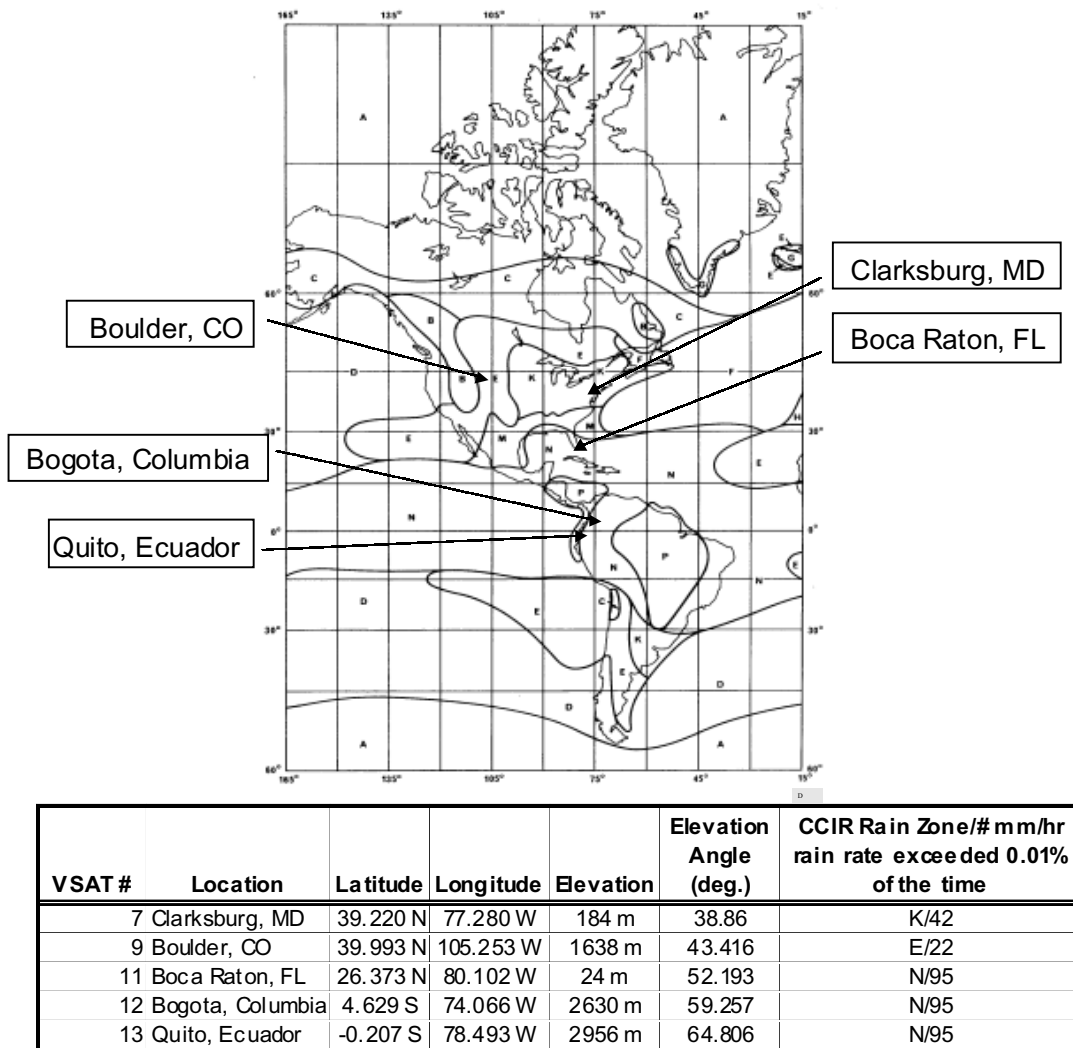


Figure 2.2: Location of Five Sites for CDF in Figure 2.1.

From Figure 2.1, it can be seen that a fade of 8 dB or greater can be expected to occur only 0.01% of the time, yielding an availability of 99.99%, for a terminal located in Boulder, Colorado (a dry rain zone). A fade of 8 dB or greater will occur approximately 0.15% of the time, an availability of 99.85%, in Bogota, Columbia (a semi-tropical rain zone). In the lower fade values (0 – 2 dB) the fades are generally caused by system fades, clouds, antenna wetting, and light rain. A higher percentage of the fades in this

region occur in Boulder, Colorado than in Bogota, Columbia because of the type of environment found in each location. This is due to the higher likelihood of light rain in Colorado and because thermal distortion on the large multibeam antenna onboard ACTS (used in Colorado) is greater than on the smaller steerable antenna (used in Columbia). Thermal distortion on the multibeam antenna causes the spot beam to drift slightly, causing small fades.

2.4 Advanced Communication Technology Satellite

2.4.1 Spacecraft Description

The Advanced Communications Technology Satellite (ACTS), sponsored by the National Aeronautics and Space Administration (NASA), is an experimental satellite operating in the Ka frequency band [15]. The downlink frequency is 19.44 GHz and the two uplink frequencies are 29.291 and 29.236 GHz. ACTS is capable of operating using two modes: the Baseband Processor (BBP) mode which uses a high-speed onboard digital processor that demodulates, stores, and regenerates the baseband signals received before retransmission to the ground; and the Microwave Switch Matrix (MSM) mode, which is a dynamically reconfigurable intermediate frequency switch capable of routing high-volume traffic in a “bent-pipe” mode. The MSM channel has a maximum bandwidth of 900 MHz. The ACTS spacecraft diagram is shown in Figure 2.3.

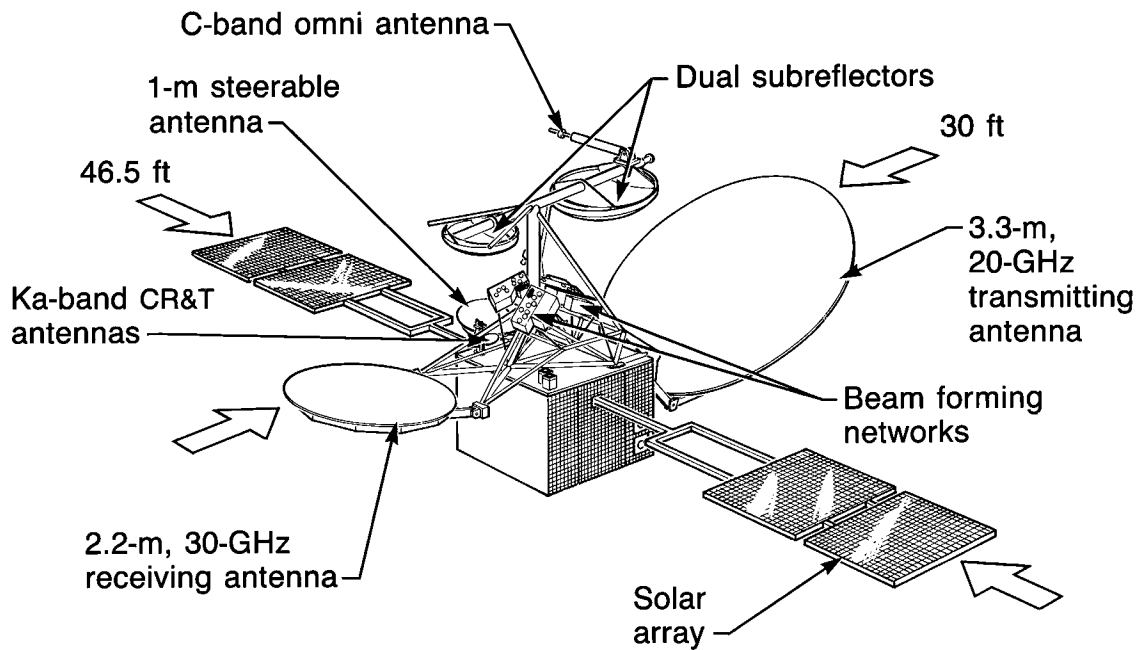


Figure 2.3: The ACTS Spacecraft.

The ACTS satellite system contains two hopping spot beams interconnected by a baseband processor using a Time Division Multiple Access (TDMA) transmission protocol. The two hopping spot beams visit up to 48 narrow spots, each approximately 200 km in diameter at the 3 dB contour. The two beams interconnect multiple users on a rapidly reconfigurable and on-demand basis. During the 1 millisecond TDMA frame, all beams with active ACTS ground stations are visited, with the beam dwelling long enough in each location to transmit and receive the required traffic (see Figure 2.4). The downlink burst rate is 110 Mbps and the uplink burst rate is 27.5 Mbps [16], [17], [18].

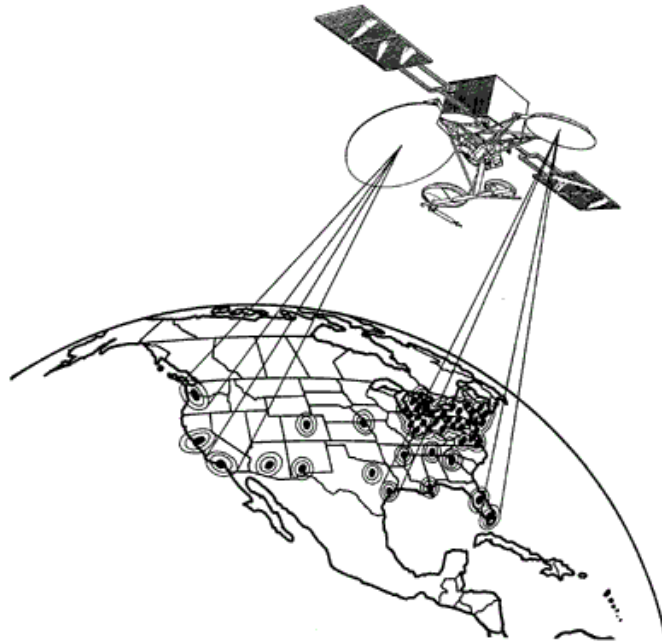


Figure 2.4: ACTS Hopping Spot Beams.

2.4.2 ACTS Communication Protocol

The 1 millisecond TDMA frame used by ACTS is divided into 1,728 equal time slots, each corresponding to the time required to transmit one 64-bit word at the 110 Mbps clock rate. A T1 Very Small Aperture Terminal (T1 VSAT) can transmit up to 28-64 kbps traffic channels, providing for a maximum throughput of 1.792 Mbps. Figure 2.5 shows a schematic of a single 1 ms TDMA downlink frame. The uplink burst is demodulated to baseband and stored in one TDMA frame, routed according to real time traffic demand and stored again in the next frame. This is then remodulated and transmitted on the downlink in the third frame.

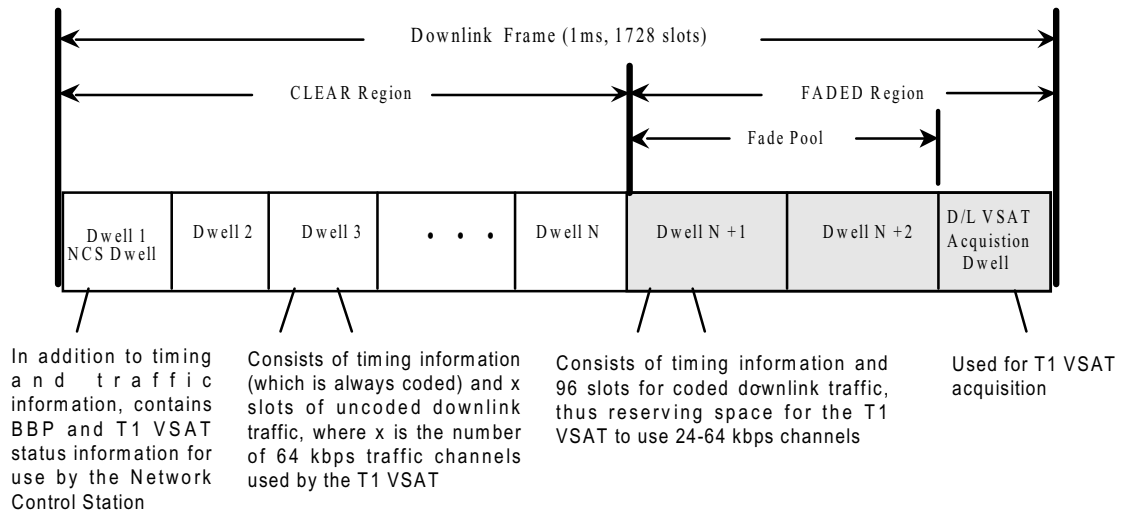


Figure 2.5: ACTS Downlink TDMA Frame Architecture.

Each TDMA frame is divided into two regions: the CLEAR and FADED region. The CLEAR region carries the timing information and traffic for each VSAT operating in the CLEAR mode (no rain condition). The FADED region is a “reserved” region, the size of which is set by the ACTS control station operators at system startup and is generally around 1000 slots. It consists of the “fade pool”, which is used to carry the timing information and traffic of VSATs operating in the FADED mode (fade compensation is enabled), as well as the VSAT acquisition window, which is used to bring VSATs into the network [19].

2.4.3 ACTS Control Network

The ground segment of the ACTS system includes the NASA Ground Station (NGS), the Master Control Station (MCS), and the Experimenter Earth Stations [20]. The NGS and MCS are co-located at the NASA Glenn Research Center in Cleveland, Ohio. The primary function of the MCS is to control the BBP communications network. The MCS performs all operation activities such as acquisition, synchronization, timing and rain fade compensation and control of all on-demand, integrated service activities such as voice, video, and data circuit connects [21].

2.5 T1 VSAT Description

The primary data analyzed for this thesis was obtained using a type of ACTS ground station referred to as the T1 VSAT. The T1 VSATs are capable of a throughput of 24-64 kbps data channels and 4-64 kbps voice channels - 1.792 Mbps total.

The T1 VSAT is the only ACTS user ground stations which uses the baseband processing mode of the satellite. The operational features of the T1 VSAT are given in Table 2.1.

Table 2.1: T1 VSAT Operational Features.

Uplink Burst Rate:	27.5 Mbps uncoded	13.5 Msps coded
Downlink Burst Rate:	110 Mbps uncoded	55 Msps coded
Antenna size:	1.2 m or 2.4 m	
Transmit Power:	12 W	
Uplink Frequency:	29.236 GHz and 29.291 GHz	
Downlink Frequency:	19.440 GHz	
Modulation Format:	Serial Minimum Shift Keying (SMSK)	
Power frequency doubler with Ku-band TWTA		
Dialable bandwidth on demand		

The VSAT is physically configured as two separate units as shown below: the Indoor Unit comprised of the digital processing and control subsystems and the Terrestrial Interface Equipment (TIE) and the Outdoor Unit comprised of the antenna and microwave subsystems [22], [23]. Figures 2.6 and 2.7 show pictures of the T1 VSAT Indoor Unit and Outdoor Unit.



Figure 2.6: T1 VSAT Indoor Unit.



Figure 2.7: T1 VSAT Outdoor Unit.

2.5.1 ACTS Fade Detection

In order to determine when to enable compensation, the T1 VSAT must accurately detect a fade. The T1 VSAT performs this operation by measuring the quality of the communications link [24], [25], [26]. The moving average link quality estimate is based on the received signal quality of the reference burst in the downlink to the earth station. To reduce the effects of inter-symbol interference at high SNR, only those samples without an adjacent bit transition are used in the calculation. The center bit of the 1's and 0's triplets in the coded downlink burst is sampled 9600 times in a 75 millisecond superframe. The mean-to-variance method [27], is then applied to the samples resulting in an estimated value of the signal level once every 75 ms. Each estimated value is stored in a First In First Out (FIFO) register. An average of 13 estimated values is reported to the MCS every 150 ms.

Because the reference burst data is always coded, the measured E_b/N_0 value is regarded as a coded value. To convert the measured E_b/N_0 to an uncoded E_b/N_0 , 6 dB is subtracted from the measured value to represent the "uncoded" E_b/N_0 value. "Coded" data represents half rate (55 Mega Symbols per Second (MSPS)) versus 110 Mbps for uncoded data. Reducing the rate in half results in a 3 dB increase in E_b/N_0 , and the remaining 3 dB results from sending each symbol twice. The reference burst data used for estimating the E_b/N_0 value does not enter the Viterbi decoder as does the coded communication data, creating a need for an additional adjustment when analyzing the coded E_b/N_0 .

Because of differences in the production of VSATs discovered at system test, a configurable “correction factor” is introduced in software. At the system test of the production units, the noise level was set at the input to the demodulator. Then an E_b/N_0 of 12.3 dB was chosen, and the corresponding signal level was calculated. The signal level was set using the same power meter as that for the noise level setting. Then the modem chassis boards were adjusted until the BER tester registered as close as possible to 5×10^{-7} (the theoretical value at $E_b/N_0 = 12.3$ dB). The correction factor is then determined so that the E_b/N_0 reading on the VSAT screen equaled 18.3 dB. This correction factor ranged from 0 to 2 dB.

An experiment using the Modem Processor Test Set (MPTS) was conducted to determine the accuracy of the E_b/N_0 estimation process [28]. Based on this experiment, the estimated E_b/N_0 value in the range of 12 – 20 dB is accurate within approximately 1 dB. For values above 20 dB, the reported value falls significantly below the actual value. At the set value of 30 dB, the error is about 6.5 dB.

Changes in the VSAT configuration during operation can alter the reported E_b/N_0 reading. Swapping of cards in the modem chassis will cause offsets in the reported E_b/N_0 of up to 2 dB. A second known source for error is the noise floor of the Low Noise Converter (LNC). The noise floor is specified as 4 dB, but some have values of 2.5 dB, resulting in a 1.5 dB error. The error would occur if the unit used at system test had a noise floor of 4 dB, and after failing, was replaced by one with a corresponding value of 2.5 dB.

Despite inaccuracies of using the link quality estimate, the need for additional equipment to receive signal strength is eliminated, thereby reducing earth station complexity and cost. Other techniques have been proposed. For example, a proposal by Dr. Robert Manning involves using the phase error in the in-phase and quadrature component of the QPSK modulated signal to estimate the SNR [29]. This proposal has not yet been tested.

2.5.2 ACTS Fade Compensation

ACTS adaptive rain fade compensation is the process whereby a VSATs data channel BER performance is automatically enhanced during a period of signal loss due to rain attenuation. The rain fade compensation protocol provides 10 dB of margin by reducing burst rates by half and invoking rate $\frac{1}{2}$, constraint length 5, Forward Error Correction (FEC) Convolutional Coding and Viterbi decoding [30], [31]. The result is a reduction of the 110 Mbps burst rates to 55 Mps and the 27.5 Mbps burst rates to 13.75 Mps. The protocol is adaptive in that it includes a decision process so that fade compensation is implemented only when needed. This allows for the sharing of the spacecraft's decoding capacity. The decision process, which determines the need for compensation in real time, makes use of the downlink signal level, an ONSET threshold, and a CESSATION threshold [30]. The two thresholds are used to account for noise in the signal level measurement and to add stability to the decision process. The ONSET and CESSATION thresholds are set individually per VSAT based on each VSAT's BER performance.

The downlink signal level measurement is made by each VSAT and transmitted to the MCS. If the signal level falls below the ONSET threshold, the MCS instructs the VSAT to operate in the coded mode which enables compensation. Compensation remains implemented until the signal level rises above the CESSATION threshold (usually set about 1 dB higher than the ONSET threshold). Coding is applied to both the downlink and uplink data, although the decision to implement and remove coding is based only on the downlink signal level.

The specific levels at which the thresholds are set directly impact VSAT BER performance. If the thresholds are set too low, a VSAT may experience bit errors before coding is implemented. If the thresholds are set too high, the spacecraft decoding capacity may become exhausted, limiting the number of VSATs that can operate [32], [33]. Figure 2.8 depicts the E_b/N_0 values during a rain event. The dotted line shows the ONSET threshold and the dashed line shows the CESSATION thresholds [34], [35].

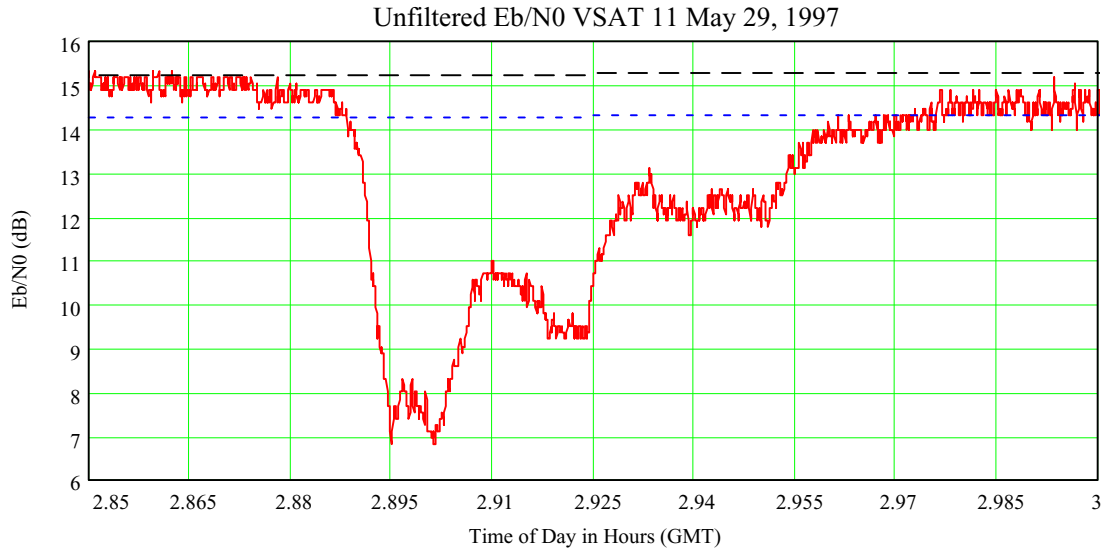


Figure 2.8: Sample ONSET and CESSATION Threshold Settings.

Each VSAT can also be configured so that coding can never be applied. This method is used when a VSAT is regularly operating below the ONSET threshold because of its location in the beam contour or because of anomalies with equipment. Compensation might be disabled for this VSAT in order to increase the amount of resources available to other VSATs.

2.5.3 ACTS Clear Sky Margins

The margin is determined by subtracting the E_b/N_0 value at “clear sky” (generally the highest value when 1 minute averaging is used to reduce scintillation effects) from the E_b/N_0 value when the BER is equal to 5×10^{-7} . The operating parameters and resultant theoretical fixed margin for a VSAT operating in Cleveland, Ohio is shown in Table 2.2. The Mathcad algorithm used to derive the stated results is given in Appendix 1.

Table 2.2: ACTS T1 VSAT Theoretical Link Budget Results in Cleveland, Ohio.

Uplink Parameters		Downlink Parameters	
VSAT Antenna Diameter	1.2 meters	Spacecraft EIRP	69.56 dBW
Uplink Frequency	29.3 GHz	Downlink Frequency	19.5 GHz
Uplink Power	12 Watts	Uplink Pointing Loss	3 dB
Uplink Pointing Loss	3 dB	Path Loss	209.792 dB
Path Loss	213.342 dB	Ground Antenna Temperature	22.17 K
Spacecraft G/T	20.96 dBW/K/Hz	Ground LNA Temperature	632.88 K
Implementation Loss	3.5 dB	Implementation Loss	3.0 dB
Modem Rate	27.5 Mbps	Modem Rate	110 Mbps
C/N ₀	102.08 dBW-Hz	C/N ₀	92.234 dBW-Hz
E _b /N ₀	14.341 dB	E _b /N ₀	18.667 dB
Fixed Margin	3.541 dB	Fixed Margin	7.866 dB

This table shows that the theoretical fixed margin for a T1 VSAT operating in Cleveland, Ohio is 3.541 dB for the uplink signal and 7.866 dB for the downlink signal.

CHAPTER III

COMPENSATION EXPERIMENT DESCRIPTION AND ANALYSIS

3.1 Hardware Connectivity

Figure 3.1 depicts the layout of the equipment and the flow of the data for the experiment conducted for this thesis. Two ACTS VSATs, labeled VSAT #7 and VSAT #11, were used. The experimental setup is located at the NASA Glenn Research Center, Cleveland, Ohio. Each VSAT was connected locally to an HP 3770B T1 bit error rate test set. A duplicate test set for each VSAT was located at the ACTS Master Control Center. Whenever these VSATs were configured to operate within the ACTS Baseband Processor (BBP) network, a 6 channel, 2-way data connection (384 kbps) was placed between the test set at the MCS and the test set at the VSAT site. This allows the uplink and downlink BER to be monitored between the MCS and the VSAT through the satellite.

Every two minutes, the BER at the VSAT site (downlink BER) and at the MCS (uplink BER) was recorded on a computer located at the MCS. The downlink BER was obtained remotely by placing a call through the satellite to the BER test set, through the VSAT modem. After these values were recorded, the BER test sets were reset.

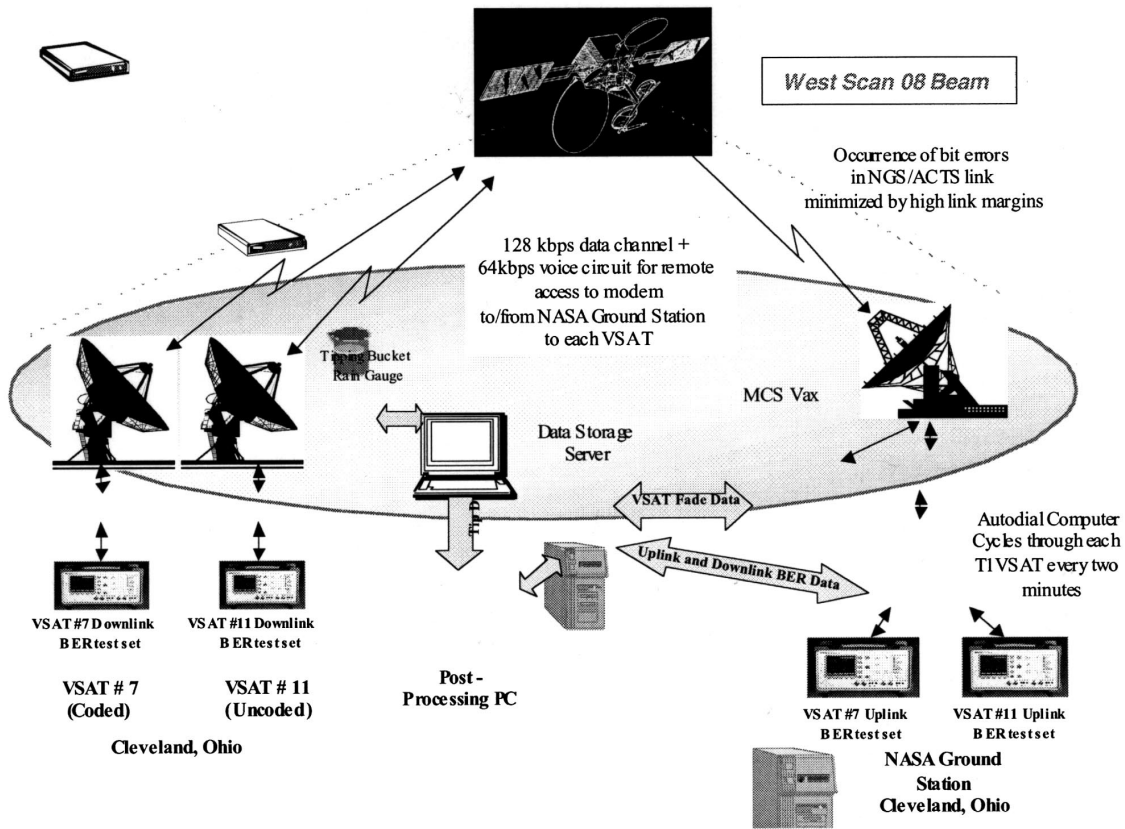


Figure 3.1: Hardware Configuration for BER Measurement.

VSAT #7 was configured to operate in the coded mode with an ONSET threshold of 14.25 dB and a CESSATION threshold of 15.35 dB. Compensation was disabled for VSAT #11.

Also co-located with the VSATs was a tipping bucket to collect rain. When the water level reaches 1/100" the bucket tipped, and a time stamp recording the time of the tip was stored on a PC. A picture of the tipping bucket and photos of the VSATs and the NASA Ground Station is shown in Figure 3.2.

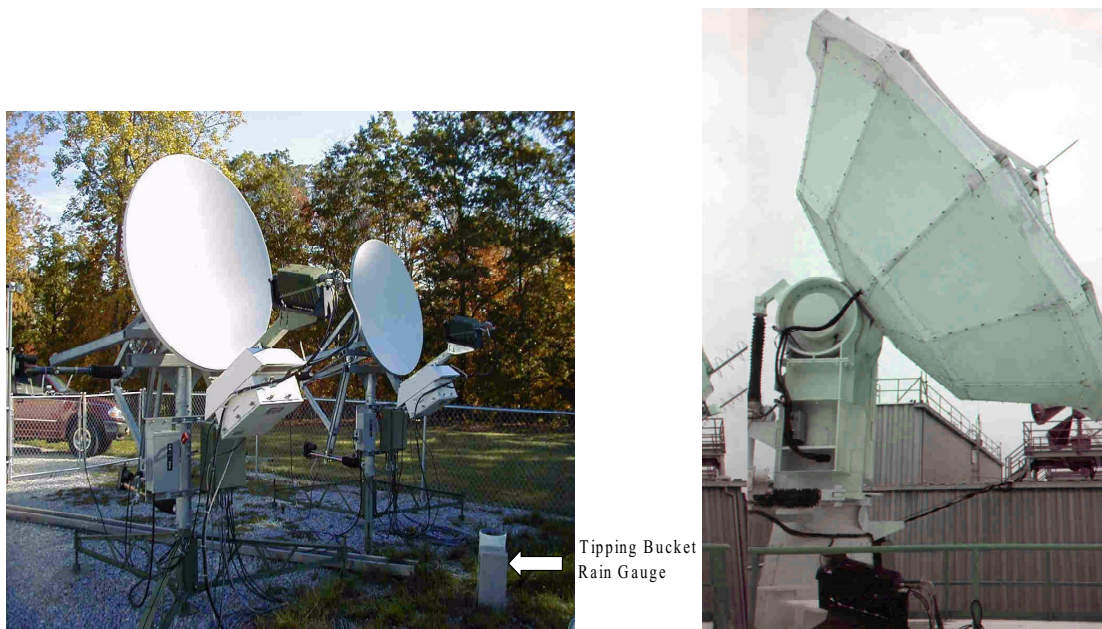


Figure 3.2: Experiment Photo of VSATs, Tipping Bucket, and Ground Station Antenna.

The raw data from the Master Control Station (MCS), including the VSAT fade data, and from the BER data are converted to tables and archived on a data storage server. This allows the data to be available over a network for post-processing and analysis. The raw data from the tipping bucket is directly transferred to the post-processing PC.

3.2 Sample of Post-Processed Experimental Data

Post-processing is implemented to obtain the E_b/N_0 , BER and tipping bucket time series data for the relevant events. These are correlated, graphed, and statistical results are obtained using the Mathcad software package. Relevant information can then be obtained from both the time series and statistical results. The statistical results provide an understanding of the amount of time a system has performed within a given operating

region. The time series results demonstrate the correlation between parameters and are used to validate the statistical results. Operating anomalies are more apparent in the time series results.

3.2.1 Correlation of Rain Event with BER and E_b/N_0

A sample time domain chart showing the tips caused during a typical rain event, the rain rate, and the corresponding fade is shown in Figure 3.3. The time of the tip is shown as a diamond on the chart and is placed at the “9” value on the Y axis for convenience. The corresponding rain rate, using the equation:

$$\text{Rain Rate} = \frac{.0254}{\text{Time}_{i+1} - \text{Time}_i} \quad (\text{mm/hr})$$

is depicted on the figure as a dashed line. The measured fade is shown as a solid line.

Figures 3.4 and 3.5 show the downlink and uplink BERs for the same sample rain event. All plots in which data from the compensation experiment are graphed will show the coded VSAT data as a solid line and the uncoded VSAT data as a “dash dot” line. The estimated time that coding was applied and removed from VSAT #7 is shown as a light dash and dark dash, respectively.

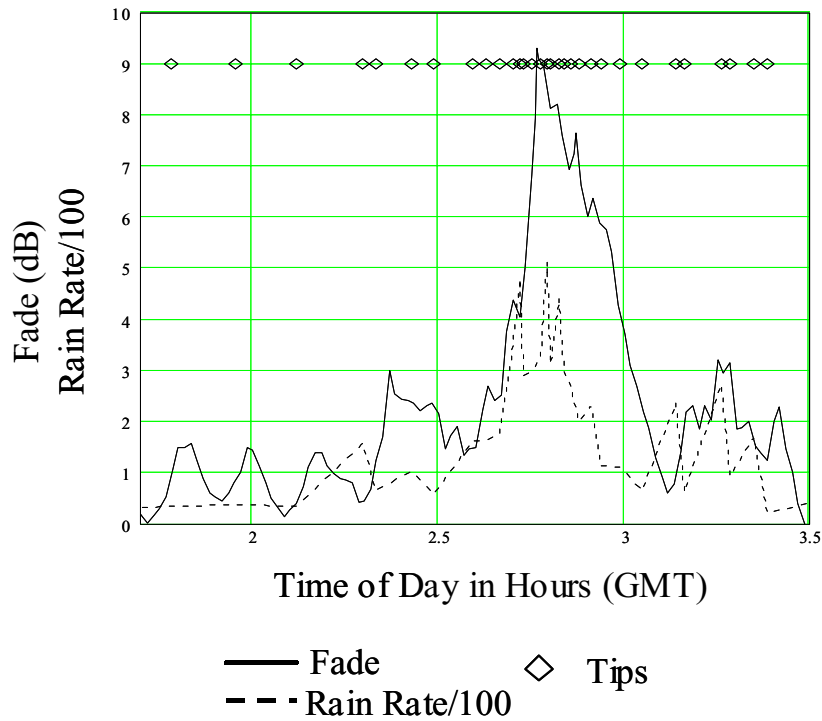


Figure 3.3: Fade and Rain Rate for Sample Rain Event.

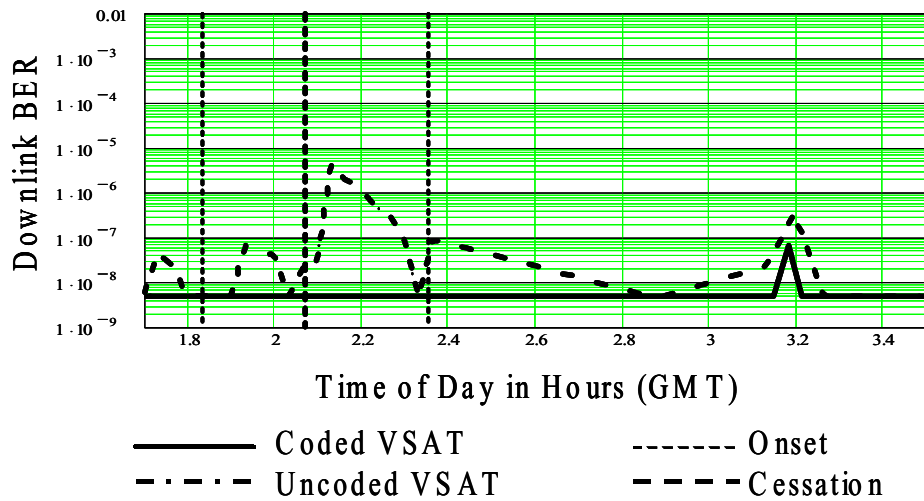


Figure 3.4: Downlink BER for Sample Rain Event.

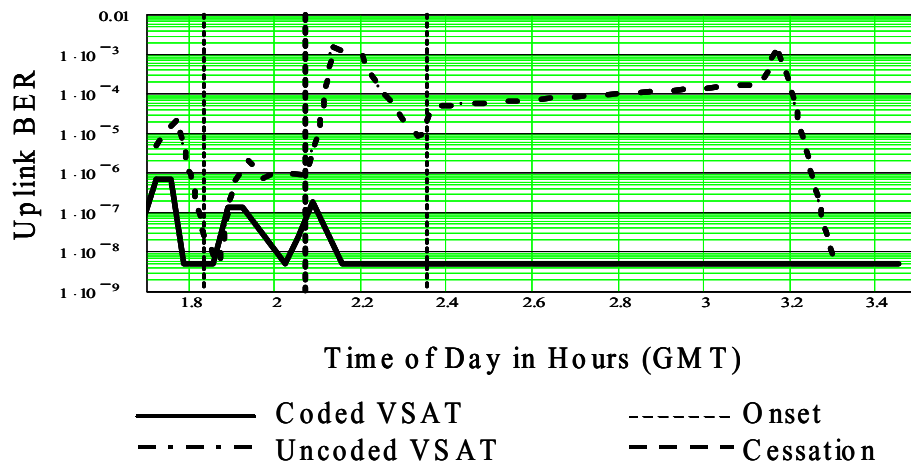


Figure 3.5: Uplink BER for Sample Rain Event.

From these charts, it can be seen that the fade rates and bit error rates generally increase with the increase in tip times, as expected. At times, this correlation does not occur because the rain might be passing through the signal path to the satellite, but it might not be raining at the VSAT location.

3.2.2 Sample Cumulative Distribution Data

Figure 3.6 depicts the cumulative distribution function of the fade data for the rain event shown in Figures 3.3-3.5 for the coded VSAT and uncoded VSAT. This incorporates approximately 2 hours of data. The coded VSAT has a larger dynamic range than the uncoded VSAT, but all other fade values should correspond. Due to equipment malfunctions and occasionally inaccurate software settings, the fade values are not aligned perfectly. From this chart, the percentage of time that a fade exceeds a certain value can be derived.

The distribution of downlink and uplink BER for the rain event depicted in Section 3.2.1 is shown in Figures 3.7 and 3.8. The limited range of obtainable BER is apparent from these curves. Downlink BER beyond 10^{-5} is not available even though the corresponding E_b/N_0 measurements were obtained. This is due to the corresponding uplink BER exceeding the limits of the BER modem's ability to receive data.

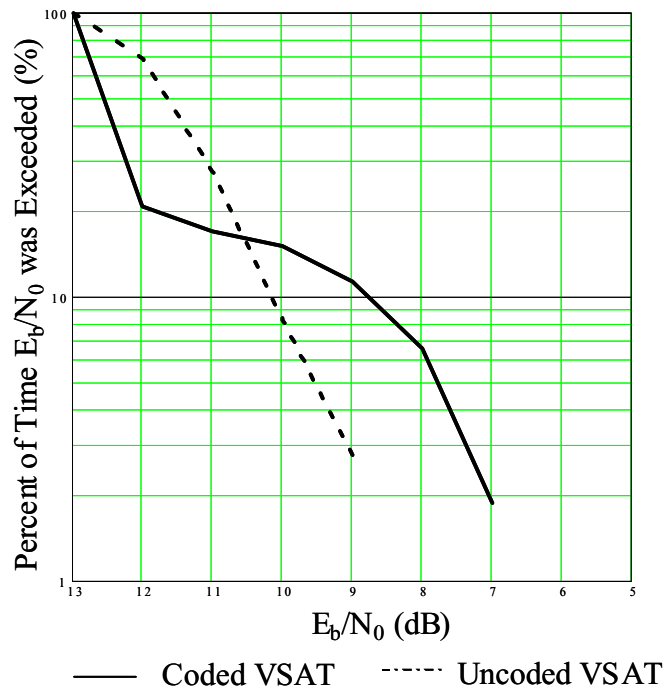


Figure 3.6: Distribution of Fade for Sample Rain Event.

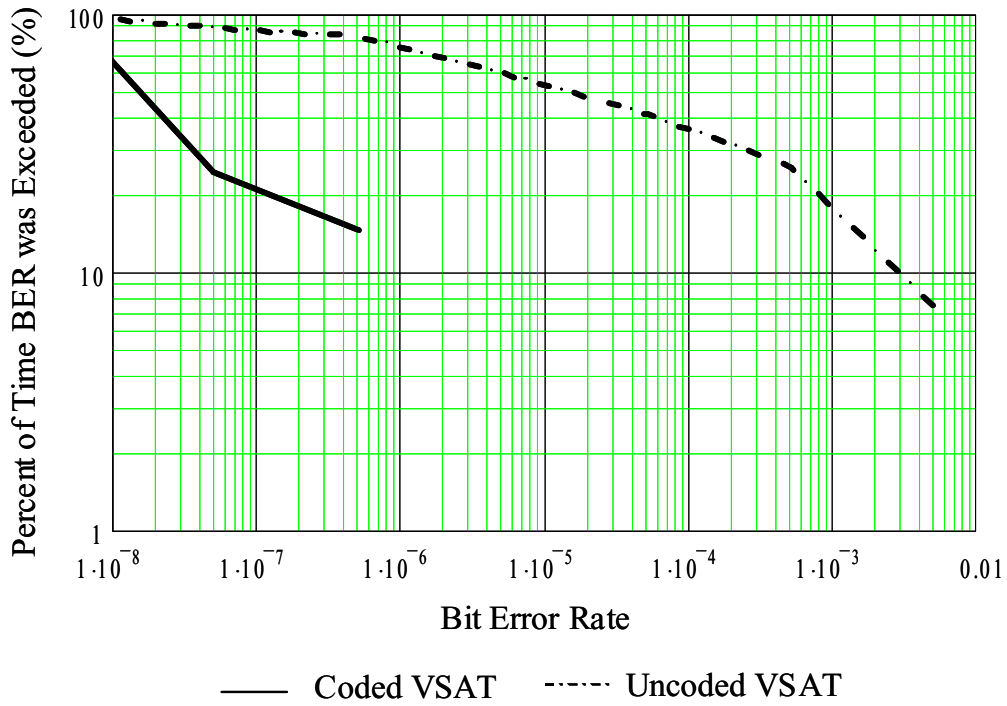


Figure 3.7: Distribution of Downlink BER for Sample Rain Event.

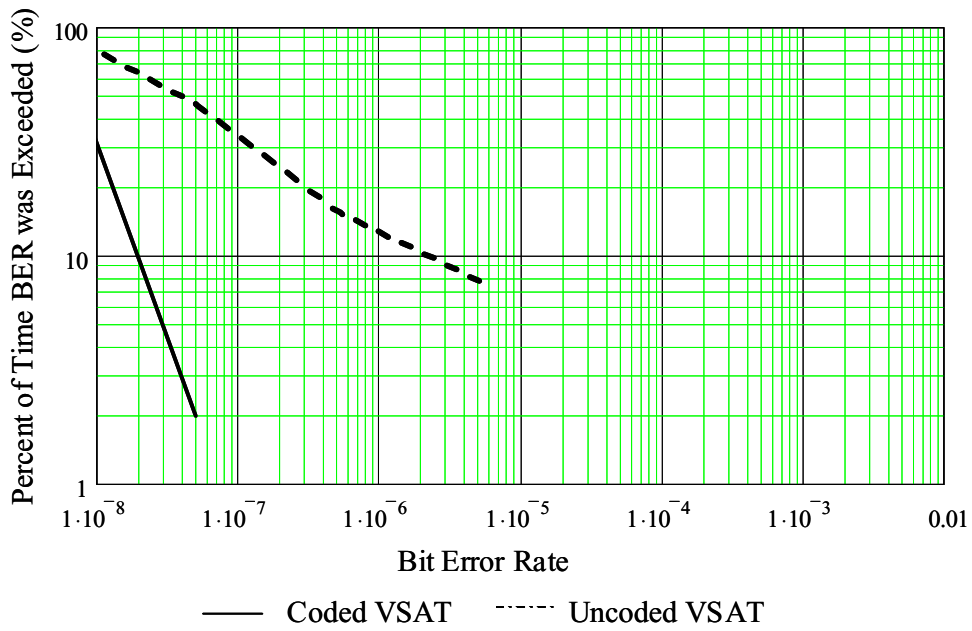


Figure 3.8: Distribution of Uplink BER for Sample Rain Event.

3.3 System Calibration

In order to obtain a controlled relationship between T1 VSAT fade values and BER readings, a calibration experiment was conducted. This calibration experiment was performed by placing both T1 VSATs' antennas in a fixed position by disabling their antenna controllers. North-south station keeping maneuvers on ACTS were suspended in August of 1998 to preserve the remaining fuel and prolong its operational life. Gravitational effects of the moon, sun, and earth cause the satellite to begin to operate in an inclined orbit. By fixing the VSAT antenna pointing to the center of the "box" within which the ACTS satellite moves, the signal slowly drifts in and out of the VSAT's antenna range, providing a large range of E_b/N_0 readings.

In order to limit the variables that might affect the E_b/N_0 value, the calibration experiment was conducted only on days when there was no rain. In addition, the experiment setup was modified so that the downlink BER was obtained over terrestrial lines, instead of over the satellite. This allowed downlink BER measurements that are not limited by the degradation of the uplink BER.

The E_b/N_0 and BER values for both the coded and uncoded VSAT are shown in Figures 3.9 – 3.11 during one "cycle" of ACTS. These charts show the extended operational range provided by coding and the effectiveness of the coding. Note that the coded VSAT loses synchronization at E_b/N_0 of about 6.5 dB while the uncoded VSAT remains synchronized until E_b/N_0 reaches 0.5 dB. Downlink BERs of 10^{-5} to 10^{-2} with the coded VSAT are also measured due to the downlink BER collection modem operating terrestrially. These correspond to measured E_b/N_0 of 1.8 dB to 0.3 dB.

Because the E_b/N_0 measuring process has not been tested in the lower ranges and is known to be non-linear, it is not expected that these values do not correspond to the theoretical values for convolutional coding. If, however, 4 dB is added to the measured E_b/N_0 value, a closer correspondence is found. This may be due to the fact that the E_b/N_0 measuring process does not pass through the Viterbi decoder, as does the BER data, which adds approximately 4 dB additional gain.

Also to be observed from the time series chart in Figure 3.11 is the amount of errors in the uplink signal when coding is removed at approximately 12.25 hours and before coding is added at approximately 15.5 hours. This is due to the fact that the thresholds are set to optimize downlink bit error rates and not uplink.

The system margin can be obtained from the calibration curves. The clear sky E_b/N_0 , obtained when the satellite reached the center of the box, is approximately 19 for VSAT #11. At the BER design specification value of 5×10^{-7} , the E_b/N_0 is approximately 11.2 dB. This gives a measured margin of 7.8 dB which closely corresponds to the theoretical margin of 7.87 dB.

Figures 3.12 – 3.14 show the cumulative distribution of the fade and the downlink and uplink bit error rates. Both the time series and statistical results show that the VSAT compensation technique complies with the design specifications.

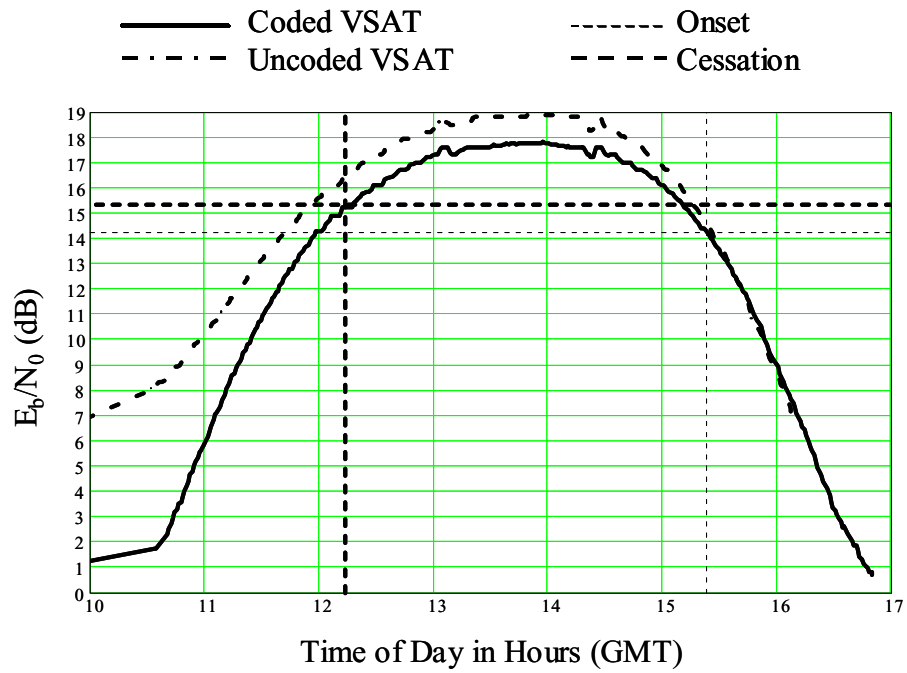


Figure 3.9: Fade Results for Calibration Experiment.

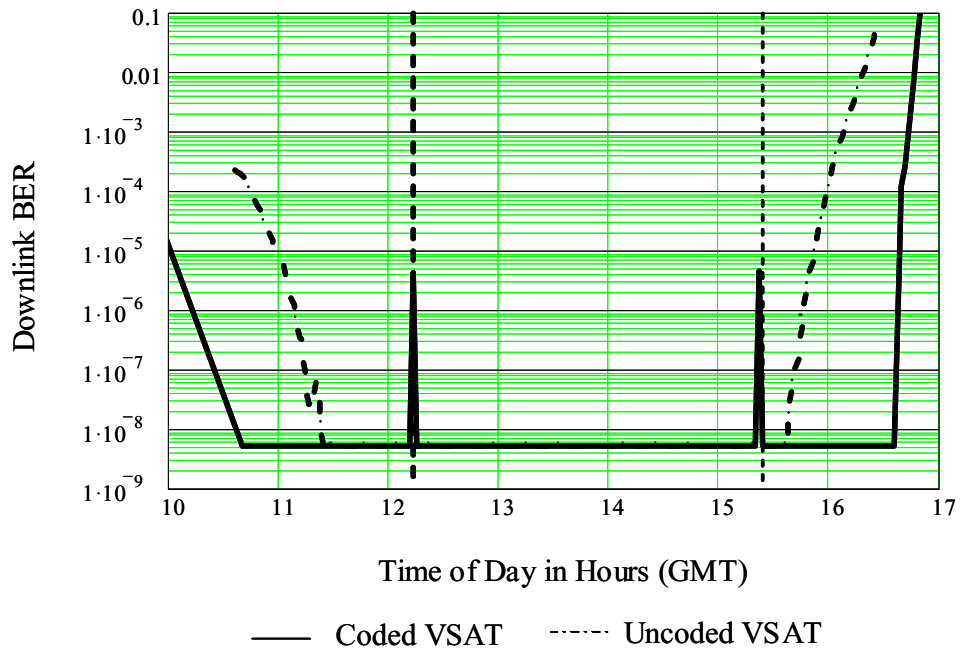


Figure 3.10: Downlink BER Results for Calibration Experiment.

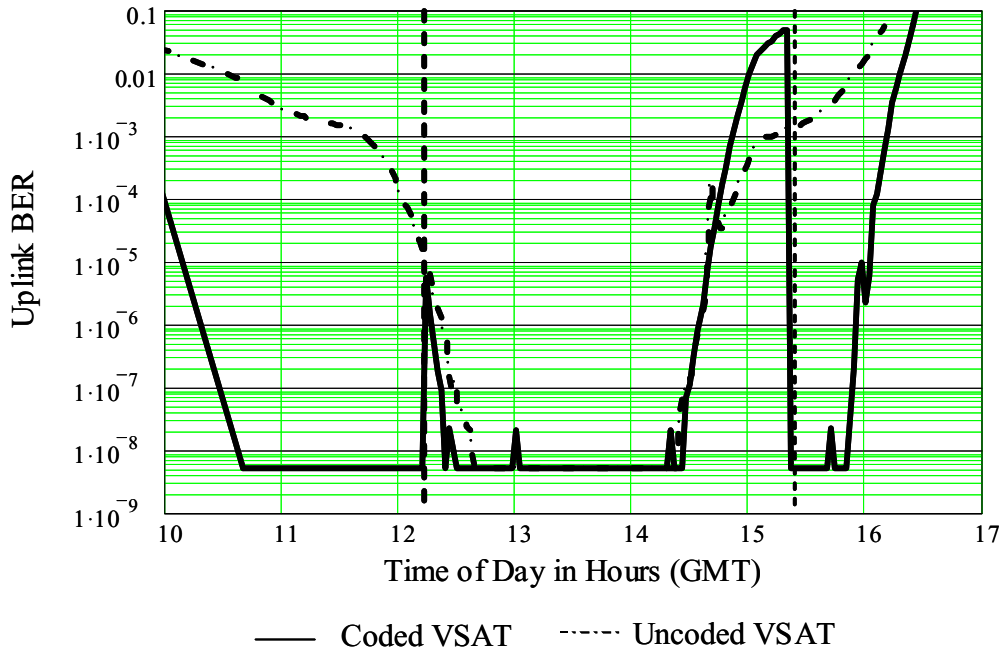


Figure 3.11: Uplink BER Results for Calibration Experiment.

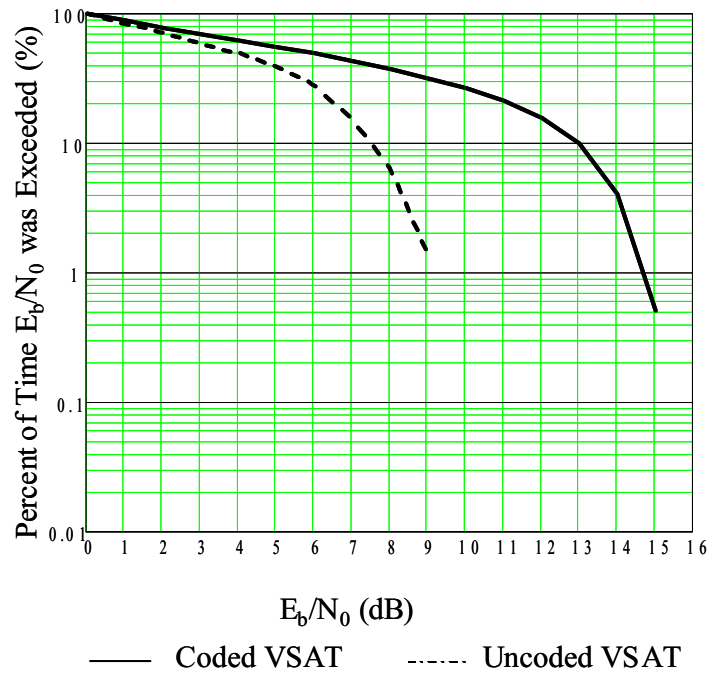


Figure 3.12: Distribution of Fade for Calibration Experiment.

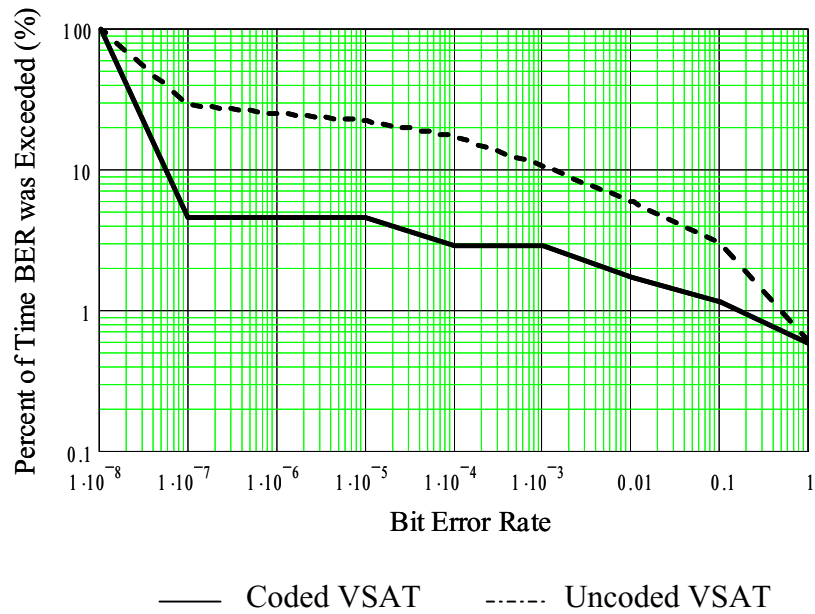


Figure 3.13: Distribution of Downlink BER for Calibration Experiment.

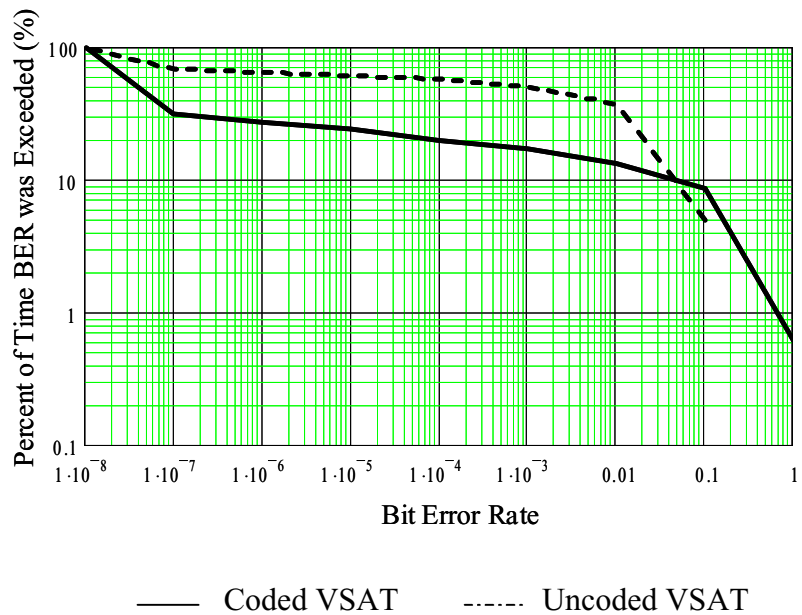


Figure 3.14: Distribution of Uplink BER for Calibration Experiment.

3.4 Compensation Experiment Data Analysis

Fade and BER data was collected during the periods of May 1999 and February 2000. Seven parameters were collected over the 10 months (3 on each VSAT and rain data) providing approximately 6 station years of data for analysis. Only days with recorded rain events are used in the analysis. This represents 97 days of the 274 days of total experimental time.

Statistical and time series analysis was performed using this data and the analysis and results are presented in this section. At the data rates which were used and the time periods for which the data was taken, any E_b/N_0 above 13 dB will have such a high BER that no bit errors will be experienced, so the BER reading during the two minute interval will be equal to zero. This zero value is changed to 5×10^{-9} in the BER database. When the uplink BER reaches 10^{-2} , the VSAT generally loses synchronization, invalidating any BER data. Therefore, the valid range of E_b/N_0 (and corresponding uncoded BER) is limited to 6 to 13 dB, which corresponds to an uncoded BER of 10^{-4} to 10^{-9} .

3.4.1 Statistical Analysis

Figures 3.15 – 3.17 show the statistical results from the compensation experiment. From Figure 3.15, it is observed that the dynamic range of the coded VSAT is approximately 6 dB higher than the dynamic range of the uncoded VSAT. Circuit connect/disconnect requests and status from the T1 VSAT are carried in a portion of the uplink TDMA frame and are designated inbound orderwires (IBOW). Because missed

IBOW messages are likely to affect the integrity of the entire VSAT network, it is not coded unless the VSAT is operating in the coded mode. If three IBOWs from a VSAT are not received by the MCS, the MCS will remove the VSAT from the BBP network, causing it to lose synchronization [33]. For this reason, the coded VSAT can remain acquired with the BBP network for an additional 6 dB over the uncoded VSAT.

Approximately 1 dB difference in fades in the low fade regions is observed. This measurement difference has been observed in other operational VSATs and is due to the different operational characteristics of the hardware. During the time that this compensation experiment occurred, VSAT #11 Feed Electronic Unit (FEU) failed and was replaced by one with a lower noise floor. A new correction factor should have been set within the VSATs configuration file to reflect the VSATs new operating point, but it was not.

For clarification, it should be noted that the experimental fade distribution should not be compared to that of a typical medium rain zone fade distribution due to the fact that only days with observed rain events are included. This limitation allows for a better opportunity to examine the characteristics of the VSATs compensation technique.

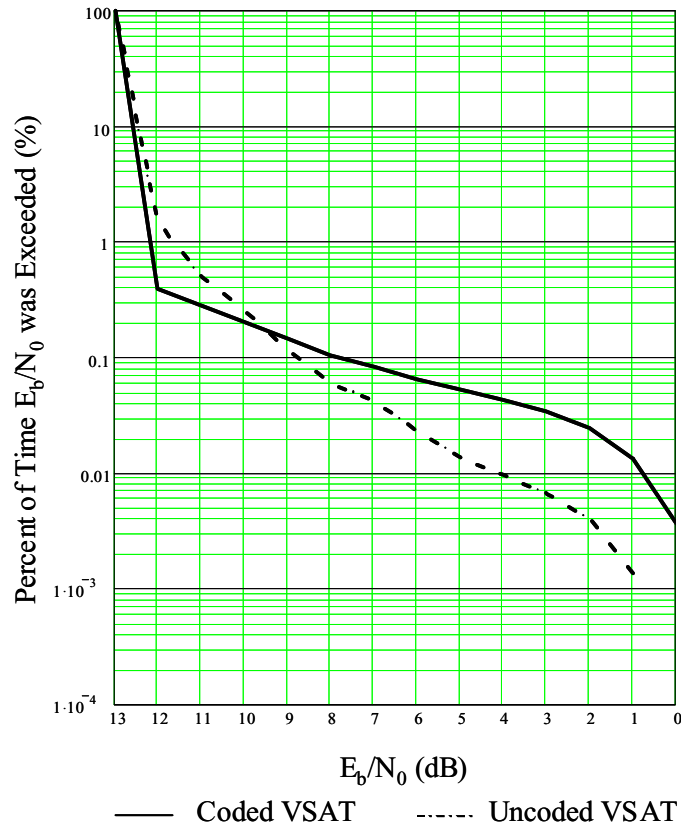


Figure 3.15: Distribution of Fade for Compensation Experiment.

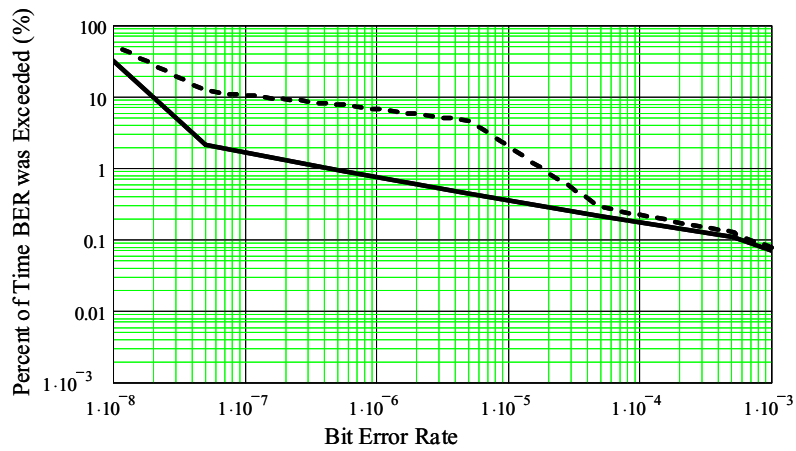


Figure 3.16: Distribution of Downlink BER for Compensation Experiment.

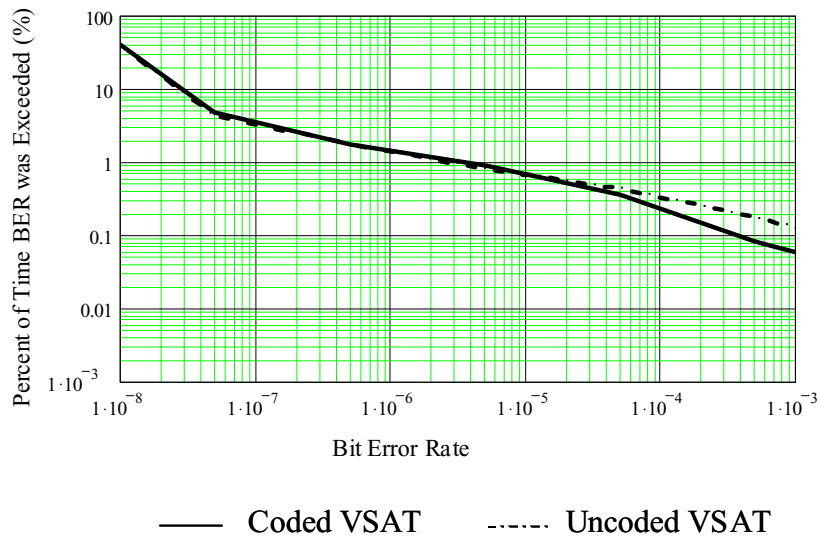


Figure 3.17: Distribution of Uplink BER for Compensation Experiment.

Figure 3.16 and 3.17 show the distribution of the downlink and uplink BER for the compensation experiment. The downlink BER improvement in the low ranges exceeds 10% between the coded and uncoded values. An anomaly with the coded VSAT #7 produced bit errors in the downlink signal temporarily when no errors should have occurred. Once the failing units were replaced, the BER returned to its expected value. In reality, the coded VSAT should experience very few errors in the limited range which it operates. Also, the characteristics of the measurement system, causing the uplink signal to lose synchronization first, and the limitations of the BER collection modem, reduces the accuracy of the BER distribution results.

Figure 3.18 illustrates the distribution of the measured rain rates. 90% of the time the rain rate fell below 42 mm/hr. This is typical for a medium rain zone.

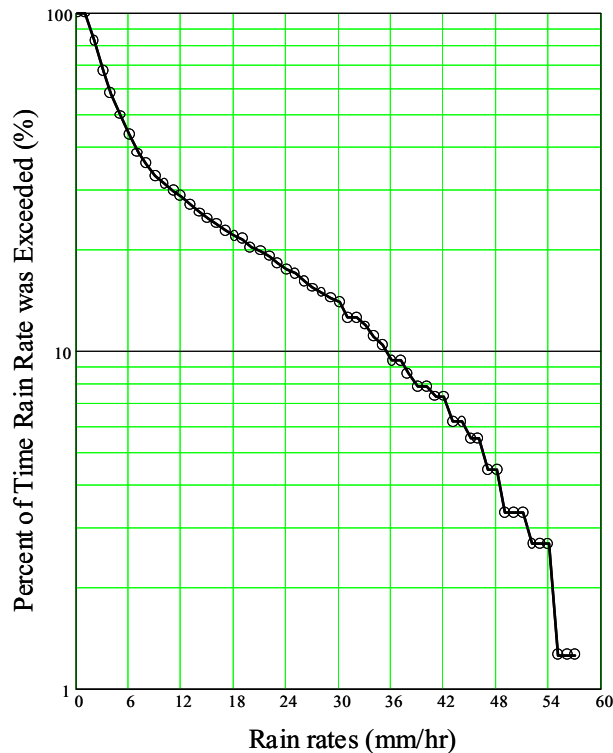


Figure 3.18: Rain Rate Distribution for Cleveland, Ohio.

3.4.2 Time Series Analysis

Figures 3.19 through 3.27 depict three typical rain events and their corresponding information. The rain rate is one factor in the value at which the VSAT loses synchronization. In addition, because the E_b/N_0 value is averaged over a one minute period, the minimum E_b/N_0 might be below the dynamic range of the VSAT but the average E_b/N_0 , as shown, would be higher.

The ability of the coded VSAT to correct for bit errors can be observed from these graphs. It can also be seen that there are no bit errors caused by the addition or removal of coding. The limitations in obtaining the downlink BER, shown by the lack of

downlink BER data when the uplink BER exceeds 10^{-3} but the VSAT is remains synchronized, is also apparent.

Figure 3.19 – 3.21 illustrate the effectiveness of the ACTS coding technique. From time 0 to approximately time 1.6, coding is enabled for VSAT #7. Although the downlink BER of the uncoded VSAT reached 10^{-6} , the coded VSAT did not experience any measurable errors in the downlink. In the uplink, the coded BER remained error-free during the rain event occurring between 0 to 2 hours. Once coding is removed at hour 3, the uplink channel experienced errors until the E_b/N_0 exceeded approximately 16.5 dB. This shows the effect of setting the thresholds on the downlink E_b/N_0 value. Increasing the downlink thresholds or the use of an additional compensation technique, such as uplink power control, could be used to compensate for the lower signal in the uplink.

The rain event depicted in Figures 3.22 – 3.24 present an interesting occurrence when the E_b/N_0 operates in the 1.2 dB region between the ONSET and CESSATION thresholds. The times depicted for ONSET and CESSATION of coding (shown as vertical lines) are approximations. Because of the averaging function, the exact times that coding was applied are not known.

Extremely close correlation between the uplink and downlink BER, E_b/N_0 , and tip times are observed in Figures 3.25 – 3.27. Overall performance during rain events shows that there are no anomalies and system specifications are met.

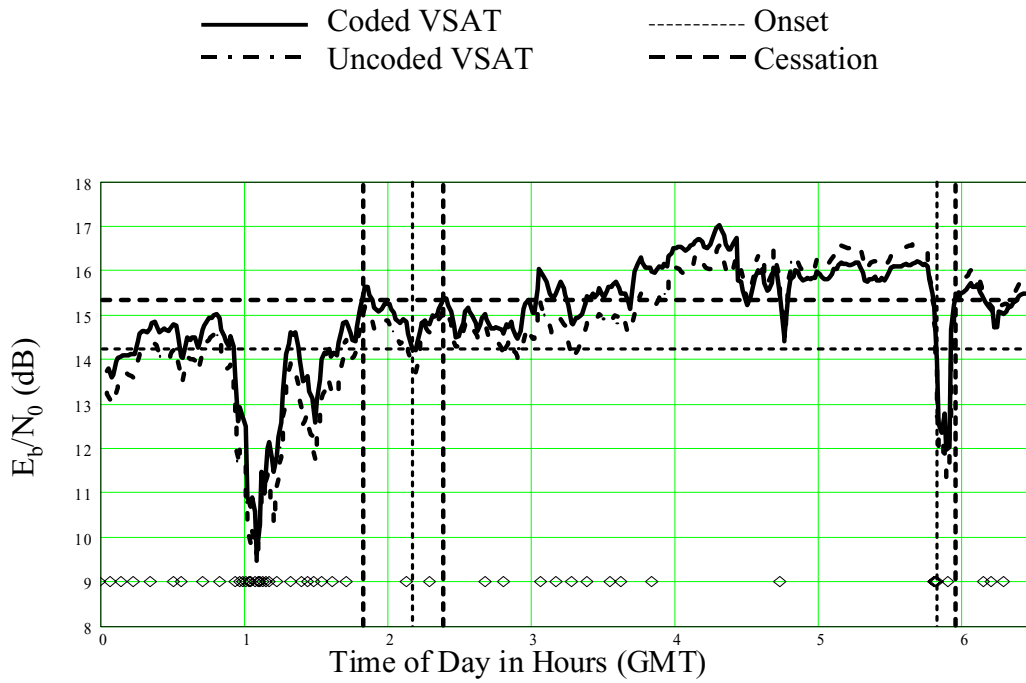


Figure 3.19: E_b/N_0 for Rain Fade Event (August 8, 1999).

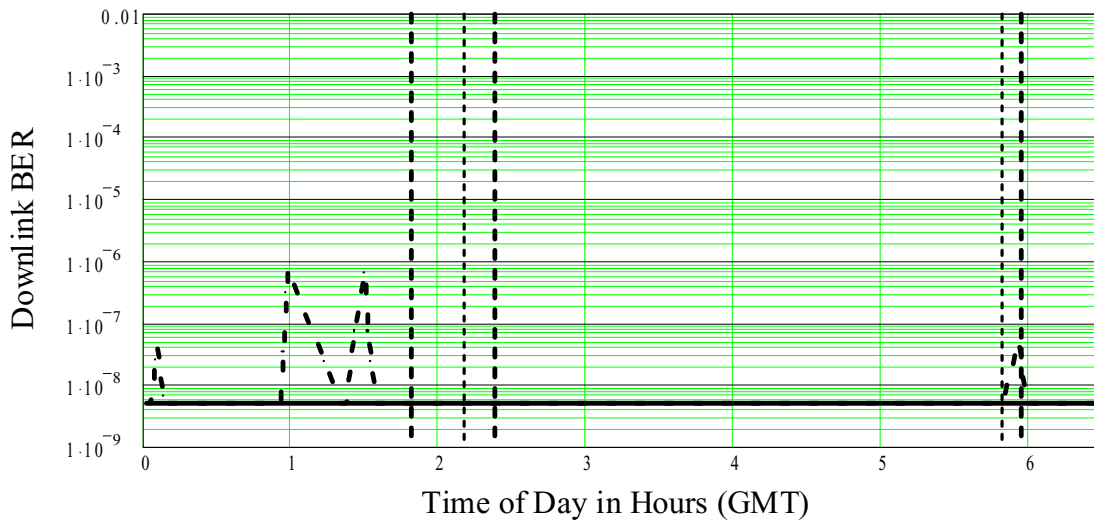


Figure 3.20: Downlink BER for Rain Fade Event (August 8, 1999).

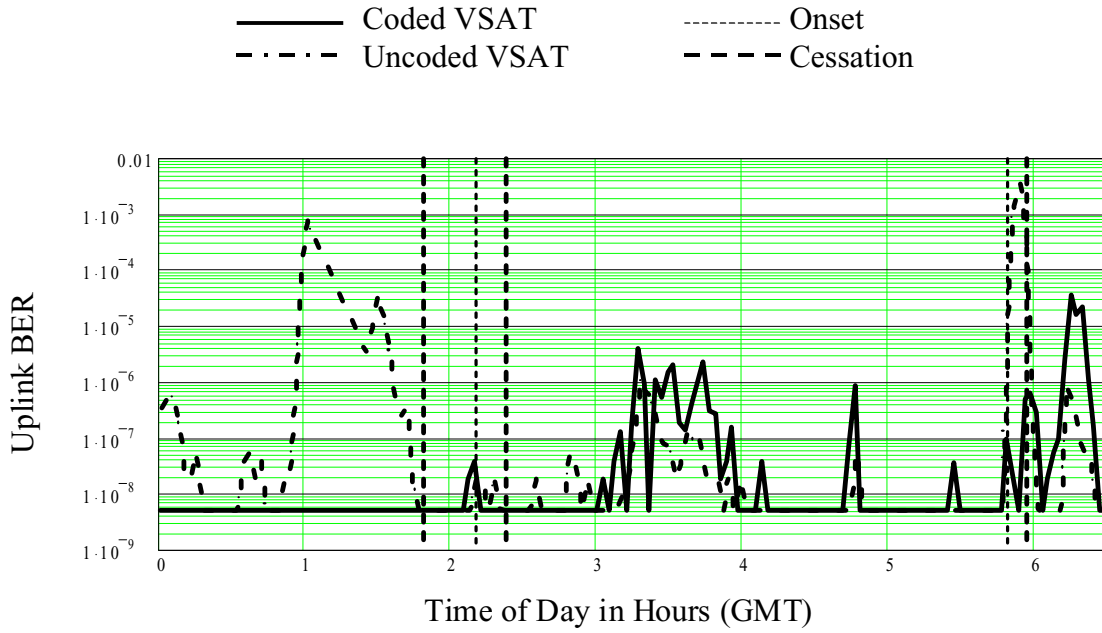


Figure 3.21: Uplink BER for Rain Fade Event (August 8, 1999).

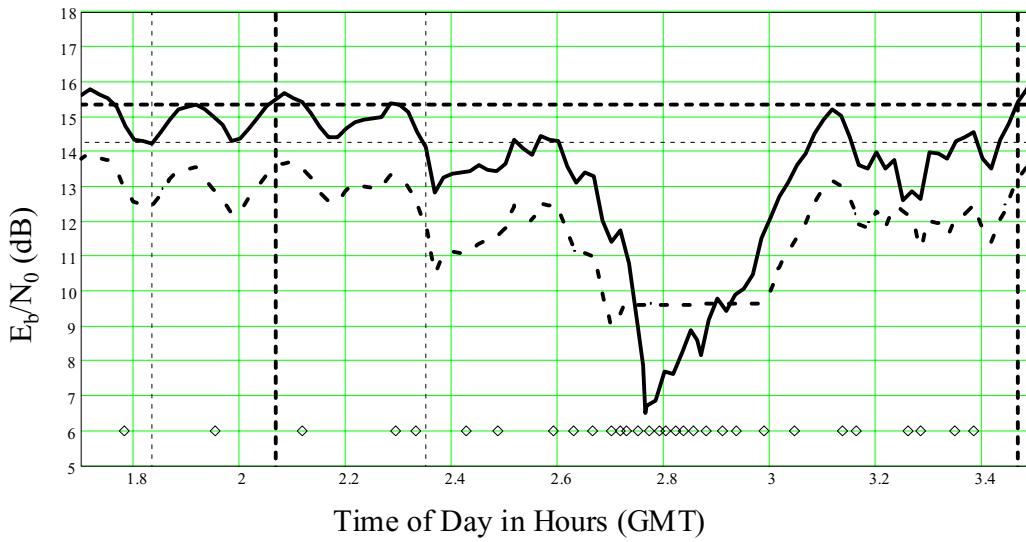


Figure 3.22: E_b/N_0 for Rain Fade Event (May 24, 1999).

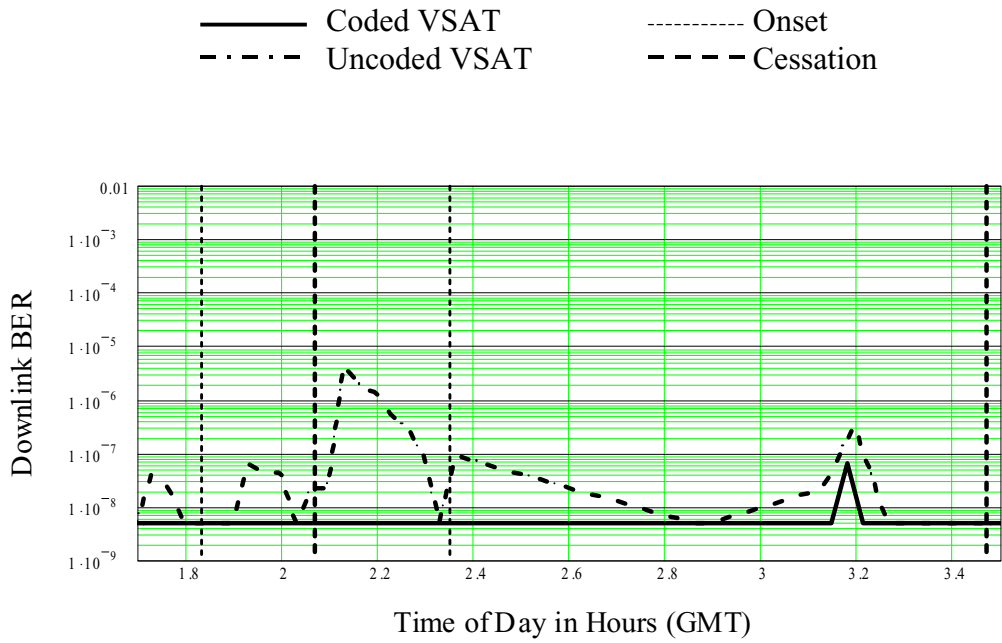


Figure 3.23: Downlink BER for Rain Fade Event (May 24, 1999).

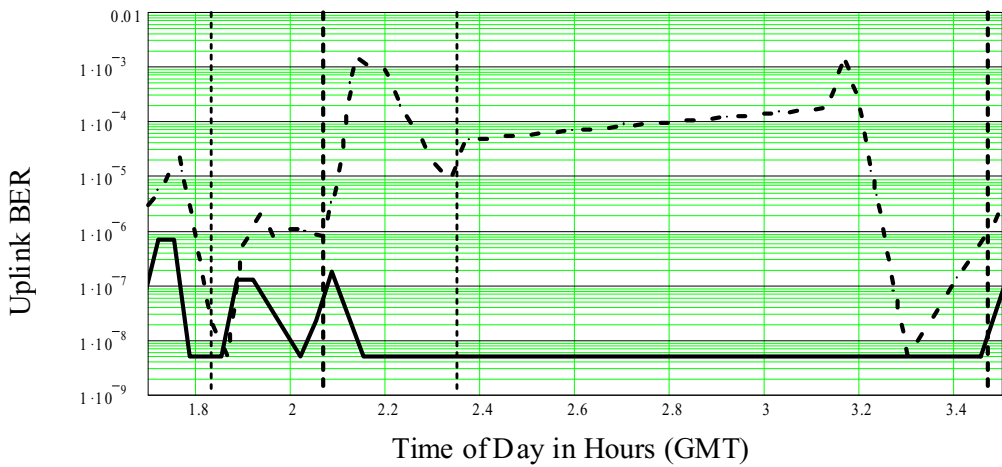


Figure 3.24: Uplink BER for Rain Fade Event (May 24, 1999).

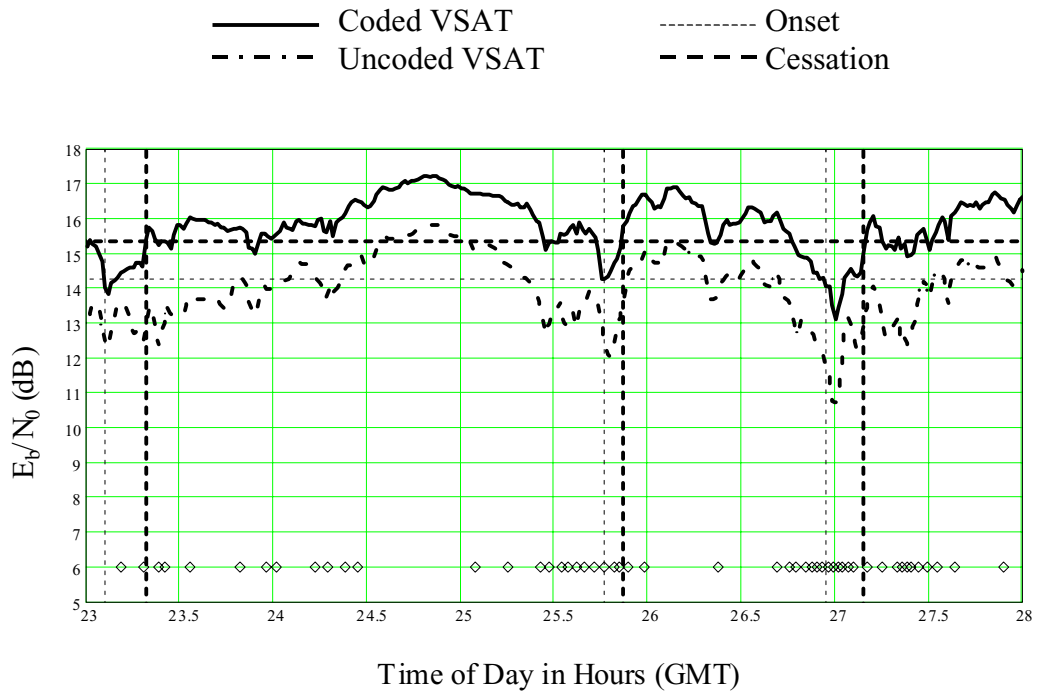


Figure 3.25: E_b/N_0 for Rain Fade Event (September 29-30, 1999).

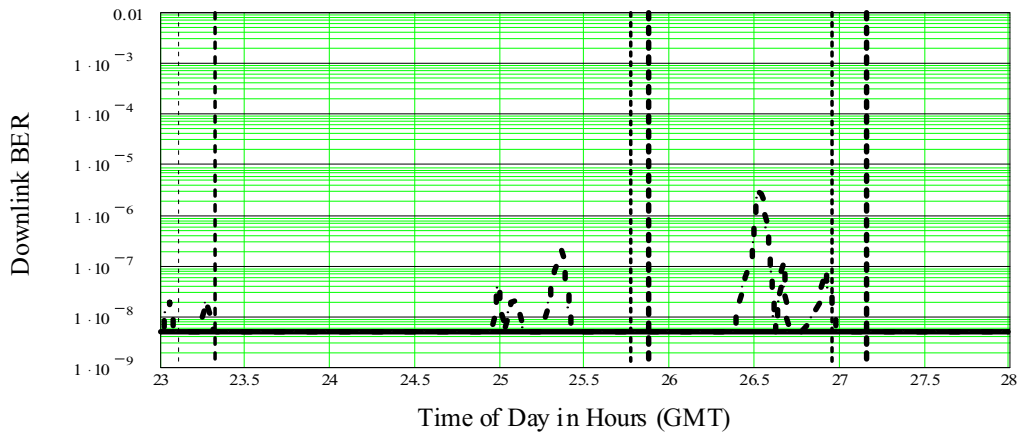


Figure 3.26: Downlink BER for Rain Fade Event (September 29-30, 1999).

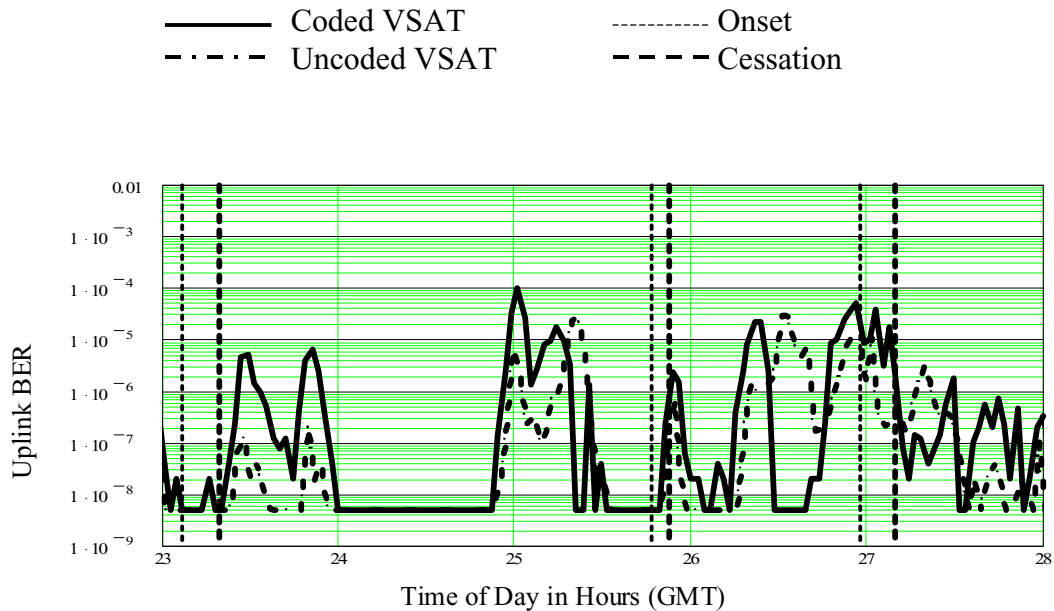


Figure 3.27: Uplink BER for Rain Fade Event (September 29-30, 1999).

3.5 Derived BER Time Enhancement Factor for the ACTS Algorithm

The measured downlink BER CDF, uplink BER CDF, and the measured BER time enhancement factor are shown in Figure 3.28, 3.29, and 3.30, respectively. The measured BER enhancement factor is found by subtracting the percent of time the coded BER exceeded a specified BER from the percent of time the uncoded BER exceeded that same specified BER. The BER time enhancement factor graph shows that the VSAT uplink availability was not increased considerably due to the addition of coding, especially in the lower BER values. This was as expected because the decision to enact coding and the threshold limitations are based on the downlink BER. The uplink BER has already exceeded the lower BER values when this decision is implemented.

The downlink BER, on the other hand, was greatly enhanced by the addition of coding. Most observed anomalies in the BER values were removed, such as inaccurate values when the VSAT first synchronizes with the network. Some invalid points do remain. If all invalid points were removed, there would be very few coded BER points greater than 10^{-7} , and the enhancement factor for BER values in the 10^{-7} to 10^{-4} range would be approximately equal to the uncoded BER availability.

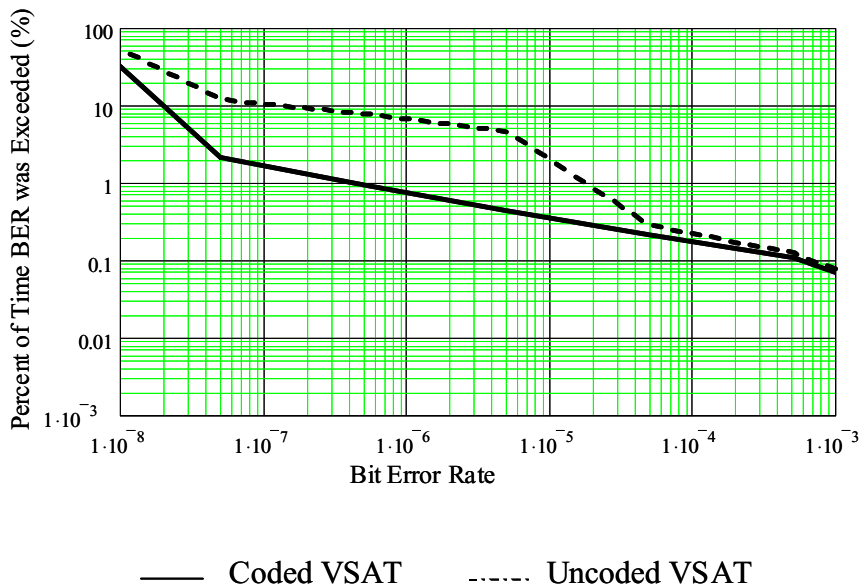


Figure 3.28: Distribution of Downlink BER for Compensation Experiment.

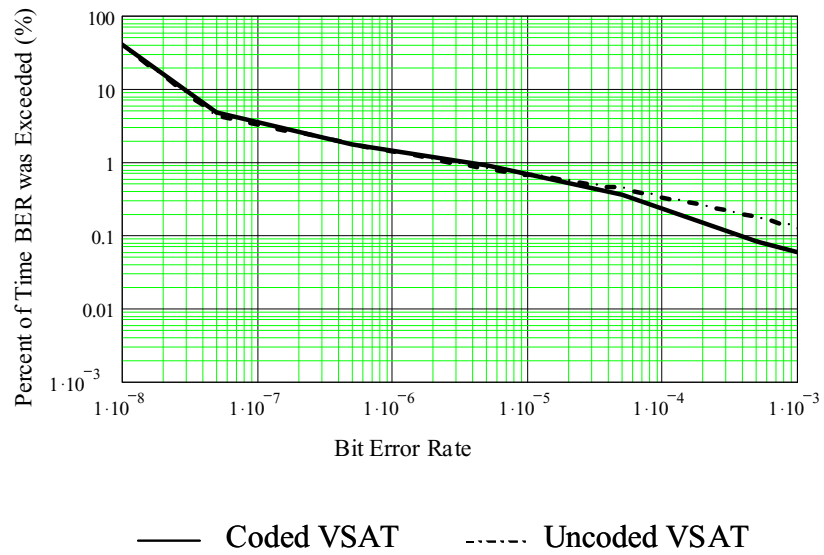


Figure 3.29: Distribution of Uplink BER for Compensation Experiment.

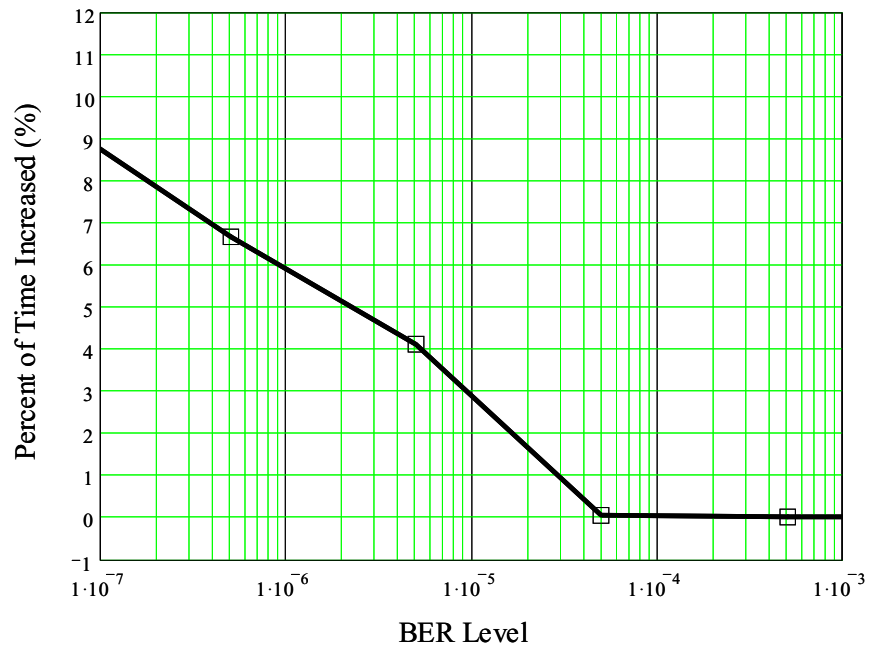


Figure 3.30: Measured BER Time Enhancement Factor.

3.6 Summary of Compensation Experiment Results

The results from the compensation experiment show that the ACTS rain fade compensation technique complies with its design specification with no observed anomalies. Statistical and time series analysis was performed using six station years of data. The time series information is presented and analyzed to validate the statistical results. Margins are calculated using a calibration experiment showing that the measured and theoretical margins are very close.

The 10 dB of adaptive link margin provided by data compensation provides 6% additional downlink BER availability in the region of interest. Additional uplink BER availability is provided at the higher BERs because of its higher carrier frequency. The results also show that the fixed margin of approximately 3 dB in the downlink and 5 dB in the uplink is adequate for most rain fades.

Limitations of the E_b/N_0 detection and compensation technique used by ACTS restrict the measurable results. The ACTS VSAT system has a limited dynamic range due to the method used to synchronize the VSAT with the TDMA network. Averaging of the fade values over a one minute interval restricts the ability to observe the exact rate of the fade and actual timing for the adaptive coding implementation. The E_b/N_0 detection and estimation process used by ACTS has known inaccuracies. Decision for uplink coding is made based on the measured downlink E_b/N_0 value and no method is available for obtaining the actual uplink E_b/N_0 .

In addition to the limitations in the ACTS technique, the configuration of the experiment conducted to validate the technique also produced restricted results. The

BER measurement system used caused incomplete downlink measurements. The difference in resolution of the E_b/N_0 measurement and BER measurements creates some degree of uncertainty. The threshold settings are not optimized for uplink data.

CHAPTER IV

DERIVED TECHNIQUE FOR FUTURE SYSTEM ANALYSIS

4.1 Bit Error Rate Time Enhancement Factor

The bit error rate time enhancement factor is the additional percent of time which a coded link will maintain or exceed a given BER level over a link system that is not coded. Once the BER cumulative distribution function for coded and uncoded operation is obtained, the BER time enhancement factor can be obtained by subtracting the availability of the coded system from the availability of the uncoded system at selected bit error rates. The BER cumulative distribution function can also be derived from the fade cumulative distribution function and the performance curves. This method is explained in the sections that follow.

4.2 Software Model

A software model has been developed to determine the BER time enhancement factor based on the particular environment, modulation and compensation technique. This allows the system engineer to determine whether adding compensation to a system can improve the availability to meet required specifications. The Simulink block diagram used to obtain the coded performance curve is given in Appendix 2. The MATLAB code developed to process the software model is given in Appendix 3.

This model requires the following inputs:

1. Measured data or propagation model data of the fade CDF.
2. Link calculation for the clear sky E_b/N_0 value.
3. The probability of error for the coded and uncoded modulation scheme.
Either the probability equation or an array, derived from a communication model using a program such as SIMULINK, can be used.

Given this input, the BER enhancement factor is created using the following steps:

1. If an array was used for the system curves, a 4th order polynomial is generated for the coded and uncoded functions for the range of E_b/N_0 values that are being considered.
2. The fade from the fade CDF is converted to E_b/N_0 by subtracting the fade value from the clear sky E_b/N_0 .
3. Using the polynomials or the equation, the corresponding coded and uncoded BER distribution using the fade distribution is obtained from the system curves.
4. For the range of BER enhancements being considered, the expected coded and uncoded availability is found.
5. The BER time enhancement factor for the selected values of error is obtained by subtracting the coded BER availability from the uncoded BER availability value.

4.3 Results from Software Model using APT Data

Using the measured results from the 7 APT data, the BER time enhancement factors for each site is derived. Figure 4.1 shows the location of the seven APT sites superimposed on the ITU-R climate zones. Table 4.1 lists these sites with their geographical attributes [6].

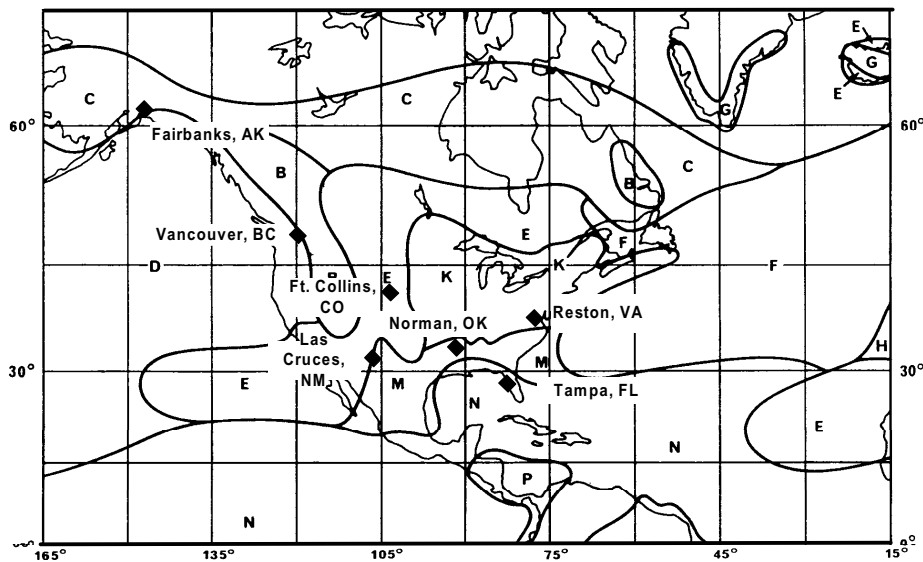


Figure 4.1: Location of Seven ACTS Propagation Terminals.

Table 4.1: ACTS Propagation Measurement Sites.

Location	ITU-R Rain Zone	Lat. (North), deg.	Long. (West), deg.	Az. From North, deg	Path Elevation deg.
Vancouver, BC	D	49	123	150	30
Ft. Collins, CO	E	40	105	173	43
Fairbanks, AL	C	65	148	129	9
Reston, VA	K	39	77	214	39
Las Cruces, NM	M/E	32	107	168	51
Norman, OK	M	35	97	184	49
Tampa, FL	N	28	82	214	52

The distribution of rain for each of these locations is shown in Figure 4.2.

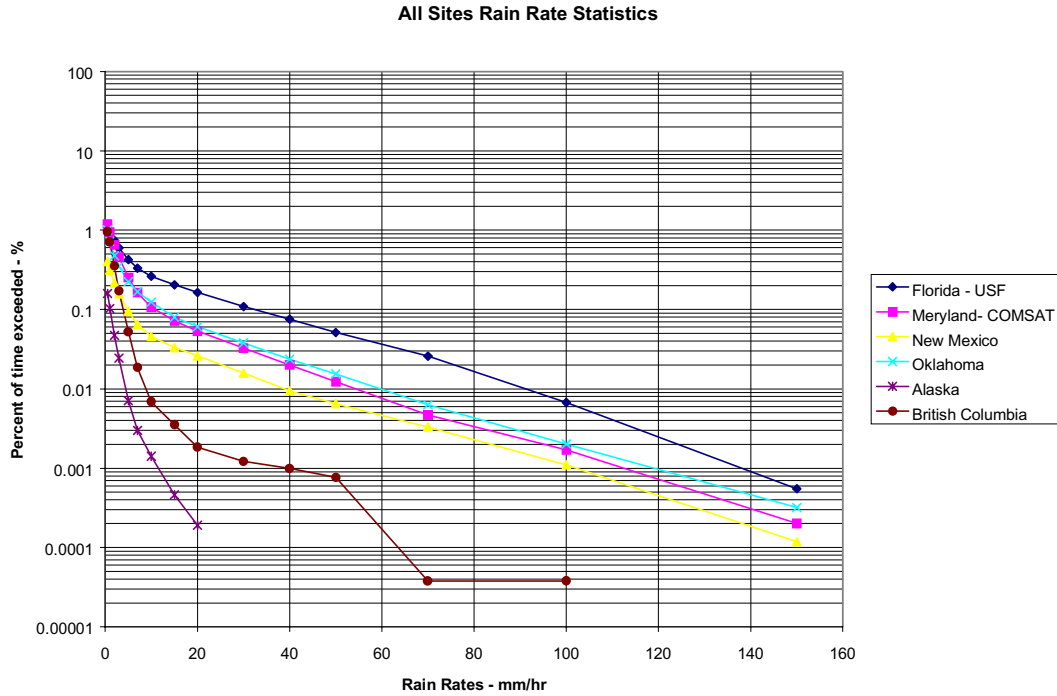


Figure 4.2: Distribution of Rain for Seven ACTS Propagation Terminals.

Example Inputs:

1. The APT fade CDF is shown in Figure 4.3.
2. The clear sky E_b/N_0 for this example is 15.3 dB. This value was chosen to be the same as the compensation experiment clear sky E_b/N_0 .
3. The performance curves for uncoded BPSK and coded BPSK with rate $\frac{1}{2}$, Constraint Length 5 Convolutional Coding is shown in Figure 4.4.

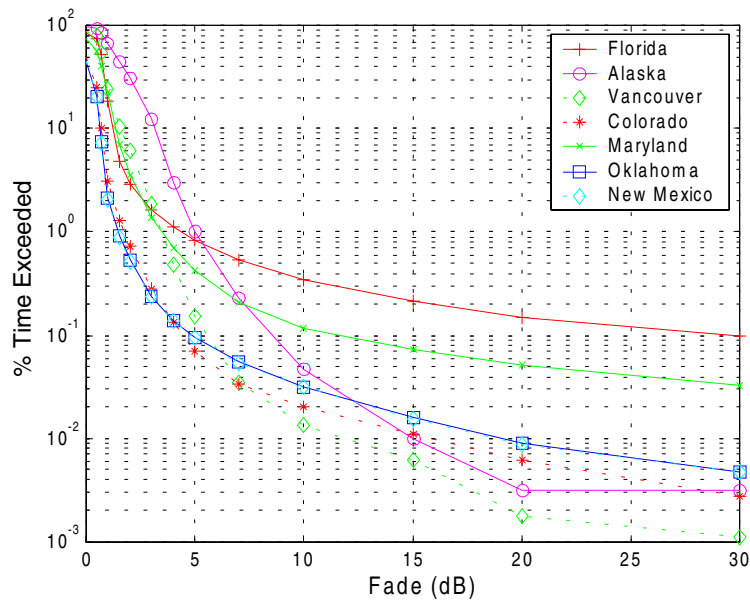


Figure 4.3: CDF of Fade using ACTS Propagation Terminals at 20 GHz.

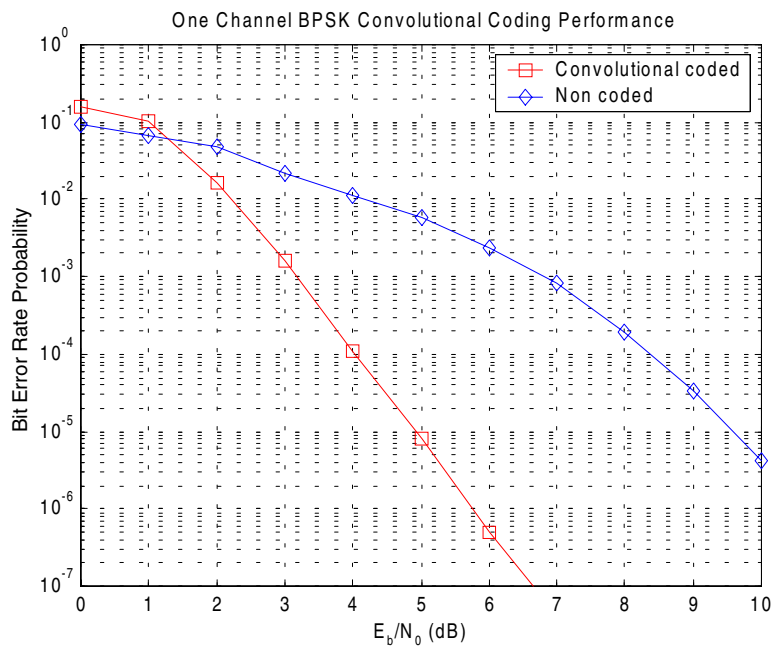


Figure 4.4: Performance of Uncoded and Coded BPSK.

The output, based on the listed inputs, is shown in Figure 4.5.

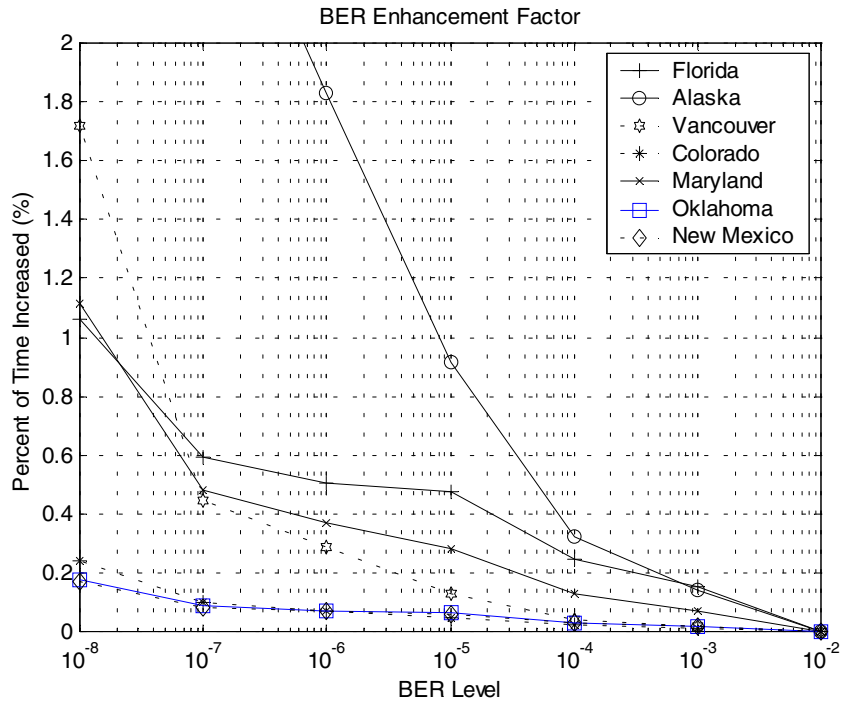


Figure 4.5: BER Time Enhancement Factor using ACTS Propagation Terminals.

From this figure, it can be shown that coding only adds approximately 0.2 % additional availability for bit error rates exceeding 10^{-8} for dry rain zones such as Colorado, New Mexico, and Oklahoma. The Teledesic satellite system objective is to perform at a BER of 10^{-9} or greater 99.99% of the time [36]. The Spaceway/Galaxy system proposed by GM Hughes Electronics Corporation specify an end to end availability of 99.5% for a BER of 1×10^{-10} [37]. In such cases, gaining 0.1% additional availability from coding can be significant.

It appears that coding can greatly enhance the availability in Alaska; however, the types of fades experienced in Alaska are due largely to the low elevation angle with respect to the ACTS altitude. This low elevation angle causes scintillation in the fade, which is a fast varying event. Scintillation effects cannot be corrected by adaptive coding, and adjusting the fixed margin to compensate for these events may be a waste of resources. The APT located in Vancouver also experiences this phenomena [38].

This result demonstrates that sites in mid-Atlantic and sub-tropical rain zones such as Maryland and Florida, can best be enhanced by coding. With coding implemented in similar zones, the occurrences of BER values exceeding 10^{-8} will be reduced by 1.5%.

4.4 Experimental BER Distribution

The experimental BER cumulative distribution function is shown as diamonds in Figure 4.6. Using the fade CDF from VSAT #7, the derived BER distribution is shown in Figure 4.6 as circles. From this graph, it is apparent that there is a large discrepancy between the two distribution functions for both the uncoded and coded bit error rates. This is expected due to the number of variables that existed in the experimental setup. Results are also affected by including the two minute averaging of BER data and one minute averaging of E_b/N_0 data, invalid data points due to equipment malfunction, and lack of BER when the BER modem did not operate. In addition, the known non-linearities associated with the E_b/N_0 estimation process leads to inaccurate BER transformation. The coded system curve for the ACTS compensation technique has not been tested in a controlled environment, and therefore the assumption was made that it

would follow the theoretical coded curve for rate $\frac{1}{2}$ Convolutional Coding with Constraint Length 5. The limited range of data, 6 to 13 dB for the uncoded VSAT and 1 to 13 dB for the coded VSAT, also limits the statistical validity of the results.

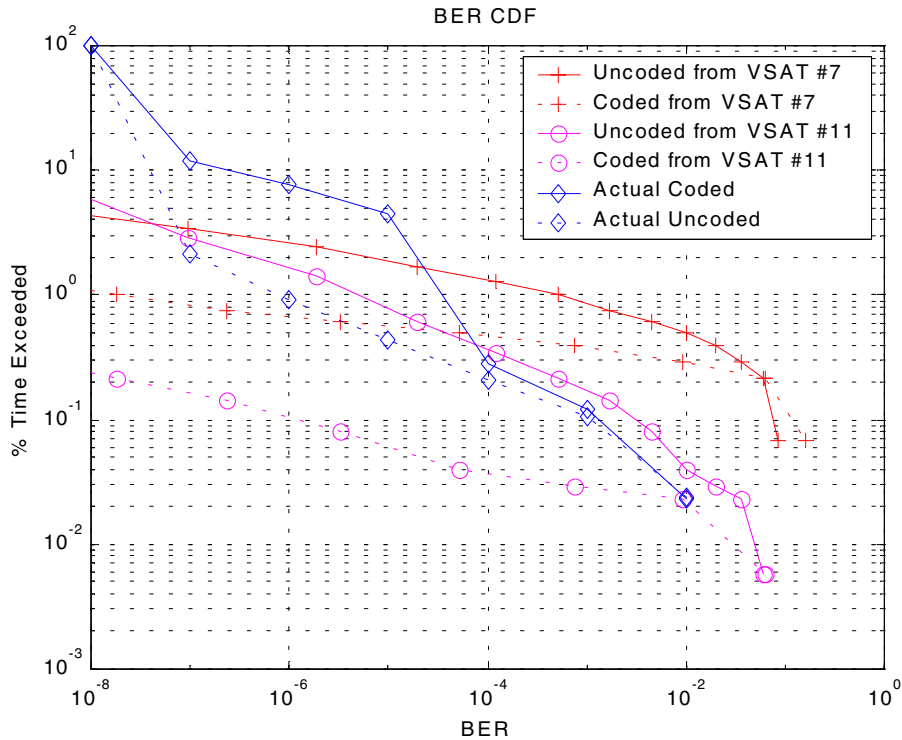


Figure 4.6: Comparison of Measured and Theoretical BER Distribution.

The measured BER time enhancement factor of at least 6% at a value of 10^{-6} is within the expected range. Because only days with measured rain events were used, the fade distribution (and therefore the BER distribution) is expected to be similar to a tropical environment. This data cannot be compared to results that might be obtained from a typical medium rain zone. A more controlled experiment with fewer variables and a coded system curve that had been characterized would allow for better comparison between actual and theoretical BER results.

CHAPTER V

CONCLUSION

5.1 Summary

In this thesis, statistical modeling and analysis of fade detection and compensation in a Ka-band satellite system has been presented using measured data from ACTS. The increased availability achieved by the compensation technique in terms of the BER time enhancement factor has been derived. The applicability of this technique has been shown using measured data from the ACTS propagation campaign. Improvements to the ACTS technique were discussed and possible implementations for future Ka-band systems were suggested.

Chapter 2 presented an overview of the ACTS system and a detailed explanation of the method used by this system to detect and compensate for fade. Chapter 3 addressed the nature of the compensation experiment setup, while highlighting the problems experienced during the experiment that limited the results. Chapter 4 presented a technique that was derived to determine the BER time enhancement factor for future system analysis.

The results show that the process developed for this thesis can assist satellite system engineers in choosing the type of modulation and coding techniques to be incorporated for their system for mitigation of rain fade. With the technique that has been validated, future system engineers can rely on estimating the expected performance for the system specifications that they are using. If additional margin is required to meet the demands of the system, additional fixed margin or other adaptive techniques can then be incorporated.

5.2 Suggestions for Improvement

The method used to estimate the SNR of the ACTS T1 VSAT inherently has limitations and non-linearities. The E_b/N_0 detection method must be reliable between units for mass production in order to allow for reliable transfer of data. Variances of less than 0.5 dB are acceptable, but the ACTS system experienced variances of up to 2 dB between production units which created inaccuracies. The E_b/N_0 detection system must be able to detect the E_b/N_0 value in less than 0.25 seconds to compensate for fades greater than 10 dB.

The threshold settings used for determining ONSET and CESSATION of coding must be optimized. This setting must be a variable parameter that is set by the system operator and dependent on the location and operating conditions of each VSAT in the network. Additional adaptive compensation techniques, such as uplink power control, would mitigate the number of uplink errors experienced when the downlink data is used to enact coding.

A method to detect the differences between system events and rain events and respond accordingly would improve the capabilities of the system. A filter to assure that the effects of scintillation do not effect the E_b/N_0 detection capabilities would also be an improvement.

Because the technique used to derive the BER time enhancement factor is based on proven theory, the results stated using measured data from the ACTS Propagation Campaign are mathematically accurate. A more controlled experiment to validate the results would be useful in the future. In this future experiment, a number of variables that existed in the past experiment and are quantified within this thesis should be eliminated. In addition, known system curves for coded and uncoded operation must be measured.

5.3 Suggestions for Implementation on Future Communication Systems

The technique used by ACTS, with the suggested improvements, would benefit the operation of future satellite systems intending to operate in Ka-band and beyond. These proposed systems, such as Teledesic [36], Astrolink [39], and Spaceway [37], use many of the technologies that allow them to make use of the ACTS techniques. During the design phases, it is critical to develop an accurate method to detect the fade in real time (within 0.25 seconds) and enact compensation. The additional costs required to design and build an adaptive data compensation technique similar to ACTS is minor compared to the cost of adding the same amount of fixed margin.

ACTS has proven that the quality of the data will not be degraded due to adaptive compensation by conducting experiments with video, voice, and data. If configured

properly, it will not overload the traffic of the system by employing adaptive compensation. This method is not relevant for systems that are operating on extremely low margins. These systems would benefit by always sending the data coded. These methods, combined with other techniques such as site diversity, can meet most availability requirements in all rain regions.

BIBLIOGRAPHY

- [1] L. Ippolito, *Propagation Effects Handbook for Satellite Systems Design*, NASA Reference Publication, Fifth Edition, February 1999.
- [2] ESA Telecommunications Program Web site:
<http://esapub.esrin.esa.it/br/br114/br114tel.htm>
- [3] Alenia Spazio Telecommunication Program Web site:
<http://www.alespazio.it/program/tlc/frtlc.htm>
- [4] R. T. Gedney, "ACTS Technology is the Most Advanced," *ACTS Quarterly Newsletter*, NASA Lewis Research Center, Issue 89/3, August 1989.
- [5] W. Stutzman, T. Pratt, C. Nunnally, R. Nealy, W. Remaklus, A. Predoehl, and A. Gaff, *ACTS propagation terminal, hardware description report*, Virginia Polytechnic Institute and State University, Virginia Tech Rep. EE SATCOM 93-3, Blackburg, VA, 1993.
- [6] F. Davarian, "Ka-Band Propagation Research Using ACTS," *International Journal on Satellite Communications*, vol. 14, no. 3, pp. 267-282, 1996.
- [7] M. Filip, E. Vilar, "Optimum utilization of the Channel Capacity of a Satellite Link in the Presence of Amplitude Scintillations and Rain Attenuation," *IEEE Transactions on Communications*, vol. 38, pp. 1958-1965, Nov. 1990.
- [8] R. C. Reinhart, S. J. Struharik, J. J. Diamond, D. Stewart, *ACTS Ka-band Earth Stations: Technology, Performance, and Lessons Learned*, NASA Technical Paper NASA/TP-2000-210047, NASA Glenn Research Center, April 2000.
- [9] J. Poiaras Baptista, G.A. Crone, A. Paraboni, D.J. Brain, "Active Compensation Techniques for Spacecraft Antennas. Part 1 – Rain Fade Compensation," *Preparing for the Future*, pp. 1018-8657, vol. 5, no. 1, March 1995.
- [10] C. Capsoni, M. Mauri, E. Martricciani, "SIRIO-OTS 12 GHz Orbital Diversity Experiment at Fucino," *IEEE Transactions on Antennas and Propagation*, vol. 38, pp. 777-782, June 1990.
- [11] A. Dissanayake, "Application of Open-Loop Uplink Power Control in Ka-Band Satellite Links," *Proceedings of the IEEE*, vol. 85, no. 6, pp. 959-969, June 1997.

- [12] A. Viterbi, "Convolutional Codes and their Performance in Communication Systems," *IEEE Transactions on Communications Technology*, vol. Com-19, no. 5, pp. 751-772, October 1971.
- [13] J. A. Heller, I. M. Jacobs, "Viterbi Decoding for Satellite and Space Communications," *IEEE Transactions on Communications Technology*, vol. Com-19, no. 5, pp. 835-848, October 1971.
- [14] A. R. Cohen, J. A. Heller, A. Viterbi, "A New Coding Technique for Asynchronous Multiple Access Communication," *IEEE Transactions on Communications Technology*, vol. Com-19, no. 5, pp. 849-855, October 1971.
- [15] F. Naderi, S. Campanella, "NASA's Advanced Communications Technology Satellite (ACTS): An Overview of the Satellite, the Network, and the Underlying Technologies," *AIAA 12th International Communications Satellite System Conference*, Arlington, Virginia, March 1988.
- [16] F. Gargione, "The ACTS Spacecraft," *AIAA 14th International Satellite Systems Conference*, Washington, D.C., March 1991.
- [17] F. Gargione, R. Acosta, T. Coney, R. Krawczyk, "Advanced Communications Technology Satellite Design and On-orbit Performance Measurements," *International Journal of Satellite Communications*, vol. 14, no. 3, pp. 133-159, 1996.
- [18] W. F. Cashman, "ACTS Multibeam Communications Package: Description and Performance Characterization," *AIAA 14th International Satellite Systems Conference*, Washington, D.C., March 1991.
- [19] C. Cox, T. Coney, "Advanced Communications Technology Satellite Adaptive Rain Fade Compensation Protocol Performance," *4th Ka Band Utilization Conference*, Venice, Italy 1998.
- [20] D. Meadows, "The ACTS NASA Ground Station/Master Control Station," *Proceedings of the 14th AIAA International Communications Satellite Systems Conference*, Washington, D.C., vol. 3, pp. 1172-1182, March 1992.
- [21] S. Struharik, D. Meadows, "The ACTS Master Ground Station Design and Performance," *ACTS Results Conference*, September 1995.
- [22] S. Johnson, "Lessons learned from ACTS T1 VSAT experiment program," *4th Ka Band Utilization Conference*, Venice, Italy, November 1998.

- [23] Harris Corporation, *LBR-2 Earth Station Statement of Work for the ACTS Program*, October 23, 1989.
- [24] R. Schaefer, R. Cobb, D. Kermicle, "Link Quality Estimation for ACTS T1-VSAT," *Advanced Communications Technology Satellite Conference*, Washington, D.C., November, 1992.
- [25] C. Cox and T. Coney, "Advanced Communications Technology Satellite (ACTS) Fade Compensation Protocol Impact on Very Small Aperture Terminal Bit Error Rate Performance," *IEEE Journal on Selected Areas in Communications*, vol. 17, no. 2, pp. 173-179, February 1999.
- [26] R. Lilley, D. Robinson, "Design Consideration on the ACTS T1-VSAT," *ACTS Results Conference*, September 1995.
- [27] K. Feher, "*Digital Communications: Satellite/Earth Station Engineering*," Prentice-Hall, Inc., New Jersey, 1983.
- [28] J. Freeman, "Final Report Concerning the Harris E_b/N_0 Algorithm," NASA Memo, May 6, 1996.
- [29] R. Manning, "A Real Time Signal-to-Noise Ration Estimation Technique for BPSK and QPSK Modulation Using the Active Communications Channel," preliminary internal communication, to be submitted as NASA Technical Memorandum, patent applied for.
- [30] P. Lowry, *Advanced Communications Technology Satellite System Handbook*, NASA TM-101490, NASA LeRC, September 1993.
- [31] Comsat Laboratories, *LBR TDMA Network Control Performance Specifications, ACTS*, ACTS-DOC-92-011.
- [32] T. Coney, "Advanced Communications Technology Satellite Very Small Aperture Terminal (VSAT) Performance," presented at the *AIAA 16th International Communication Satellite System Conference*, March 1996.
- [33] T. Coney, "Advanced Communications Technology Satellite Very Small Aperture Terminal (VSAT) Network Control Performance," presented at the *AIAA 16th International Communication Satellite System Conference*, March 1996.
- [34] Sklar, B., *Digital Communications Fundamentals and Applications*, Prentice-Hall, Inc. New Jersey, 1988.

- [35] R.E. Zieman, C.R. Ryan, “Minimum Shift Keyed Modem Implementations for High Data Rates”, *IEEE Communications Magazine*, pp. 28-37, October 1983.
- [36] “Teledesic Application with the FCC”, File No. 22-DSS-P/LA-94(840).
- [37] “Application of Hughes Communications GALAXY Inc.” before the FCC for GALAXY/SPACEWAY. FCC File Nos. 174-SAT-P/LA-95 – 181-SAT-P/LA-95. p. A-14.
- [38] C.E. Mayer, B.E. Jaeger, R.K. Crane, X. Wang, “Ka-Band Scintillations: Measurements and Model Predictions,” *Proceedings of the IEEE*, vol. 85, no. 6, pp. 936-945, June 1997.
- [39] Astrolink Web site: http://www.astrolink.com/pages/english/index_eng.html.

APPENDIX 1

LINK BUDGET FOR THE ACTS COMPENSATION EXPERIMENT

Step #1: Uplink Computations

VSAT Antenna Diameter $D_{\text{VSAT}} := 1.2 \text{ meters}$

Uplink Frequency $f_{\text{up}} := 29.298 \cdot 10^9 \text{ Hz}$

Wavelength $\lambda_{\text{up}} := \frac{3 \cdot 10^8}{f_{\text{up}}} \quad \lambda_{\text{up}} = 0.01 \text{ meters}$

Space loss $L_{\text{up}} := 10 \cdot \log \left[\left(\frac{4 \cdot \pi \cdot 37859 \cdot 10^3}{\lambda_{\text{up}}} \right)^2 \right]$

$$L_{\text{up}} = 213.342 \text{ dB}$$

Ground Antenna Gain $G_{\text{up}} := 10 \cdot \log \left[\frac{4 \cdot \pi}{\lambda_{\text{up}}^2} \cdot \left[\pi \cdot \left(\frac{D_{\text{VSAT}}}{2} \right)^2 \right] \cdot 0.55 \right]$

$$G_{\text{up}} = 48.725 \text{ dBi}$$

Uplink Power $P_{\text{up}} := 12.0 \text{ watts}$

$$10 \cdot \log(P_{\text{up}}) = 10.792 \text{ dB}$$

Uplink EIRP $EIR_{Pup} := G_{up} + 10 \cdot \log(P_{up})$

$EIR_{Pup} = 59.516 \text{ dBW}$

Uplink Pointing Loss $PL_{up} := 3.0 \text{ dB}$

Atmospheric Loss $ATM_{up} := 0.5 \text{ dB}$

Range in Km $range := 37859.0 \text{ kilometers}$

SIC Flux Density

$$FLUX := EIR_{Pup} + 10 \cdot \log\left(\frac{1}{4 \cdot \pi}\right) + 10 \cdot \log\left(\frac{1}{range^2}\right) - 60 - ATM_{up} - PL_{up}$$

$FLUX = -106.539 \text{ dBW/m}^2$

SIC Received Isotropic Power $SCIP := EIR_{Pup} - L_{up} - ATM_{up} - PL_{up}$

$SCIP = -157.326 \text{ dBW}$

SIC G/T $SCGT := 22.96 - 2 \text{ dB/K}$

Boltzman Constant $K := 228.6 \text{ dBW/K/Hz}$

Carrier to Noise Density

$$CNO_{up} := EIR_{Pup} - ATM_{up} - PL_{up} - L_{up} + SCGT + K$$

Uplink C/No $CNO_{up} = 92.234 \text{ dBW-Hz}$

Uplink EIRP $EIRP_{up} := G_{up} + 10 \cdot \log(P_{up})$

$EIRP_{up} = 59.516 \text{ dBW}$

Uplink Pointing Loss $PL_{up} := 3.0 \text{ dB}$

Atmospheric Loss $ATM_{up} := 0.5 \text{ dB}$

Range in Km $range := 37859.0 \text{ kilometers}$

SIC Flux Density

$$FLUX := EIRP_{up} + 10 \cdot \log\left(\frac{1}{4 \cdot \pi}\right) + 10 \cdot \log\left(\frac{1}{range^2}\right) - 60 - ATM_{up} - PL_{up}$$

$FLUX = -106.539 \text{ dBW/m}^2$

SIC Received Isotropic Power $SCIP := EIRP_{up} - L_{up} - ATM_{up} - PL_{up}$

$SCIP = -157.326 \text{ dBW}$

SIC G/T $SCGT := 22.96 - 2 \text{ dB/K}$

Boltzman Constant $K := 228.6 \text{ dBW/K/Hz}$

Carrier to Noise Density

$$CNO_{up} := EIRP_{up} - ATM_{up} - PL_{up} - L_{up} + SCGT + K$$

Uplink C/No $CNO_{up} = 92.234 \text{ dBW-Hz}$

Downlink Carrier to Noise Density

$$CNO_{dw} := EIRP_{dw} - ATM_{dw} - PL_{dw} - L_{dw} + GT_{dw} + K$$

Downlink C/No $CNO_{dw} = 102.08 \text{ dBW-Hz}$

Step #3: Total/Composite Computations

***Uplink C/No
(Real Number)***

$$C_{noup} := 10 \left(\frac{CNO_{up}}{10} \right)^{(-1)}$$
$$C_{noup} = 5.978 \times 10^{-10}$$

***Downlink C/No
(Real Number)***

$$C_{nodw} := 10 \left(\frac{CNO_{dw}}{10} \right)^{(-1)}$$
$$C_{nodw} = 6.195 \times 10^{-11}$$

Overall C/No

$$CNO := -10 \cdot \log(C_{noup} + C_{nodw})$$
$$CNO = 91.806 \text{ dBW-Hz}$$

Information Rate $r_{inf} := 27.5 \text{ Mb/s}$

Modem Rate (Uplink & Downlink) $r_{modup} := 27.5 \text{ Mb/s}$
 $r_{moddw} := 110 \text{ Mb/s}$

Implementation Loss (Uplink) $ImpLup := 3.5 \text{ dB}$

Non-Linear Degradation (Uplink) $NLdLup := 0.0 \text{ dB}$

Implementation Loss (Downlink) $ImpLdw := 3.0 \text{ dB}$

Non-Linear Degradation (Downlink) $NLdLdw := 0.0 \text{ dB} \quad (10^{-6} \text{ BER})$

Required Eb/No before Decoding $EbNO_{ref} := 10.80 \text{ dB}$

Downlink Eb/No

$$EbNO_{dw} := CNO_{dw} - 10 \cdot \log(r_{moddw}) - 60 - ImpLdw - NLdLdw$$

$$EbNO_{dw} = 18.666 \text{ dB}$$

Downlink Margin

$$DW_{margin} := EbNO_{dw} - EbNO_{ref}$$

$$DW_{margin} = 7.866 \text{ dB}$$

Uplink Eb/No

$$EbNO_{up} := CNO_{up} - 10 \cdot \log(r_{modup}) - 60 - ImpLup - NLdLup$$

$$EbNO_{up} = 14.341 \text{ dB}$$

Uplink Margin

$$Up_{margin} := EbNO_{up} - EbNO_{ref}$$

$$Up_{margin} = 3.541 \text{ dB}$$

Step #4: Average T1-VSAT Performance

$$a := 67.80 + 67.20 + 67.18 + 68.95 + 67.47 + 68.19 + 66.63 + 66.31 + 68.16 + 66.52$$

$$a = 674.41$$

$$b := 66.49 + 69.34 + 68.20 + 68.53 + 67.45 + 68.10 + 67.70 + 68.57$$

$$b = 544.38$$

$$\text{EIRPave} := \frac{a + b}{18}$$

$$\text{Average EIRP on the T1-VSAT} \quad \text{EIRPave} = 67.711$$

$$c := 24.65 + 23.05 + 22.53 + 23.85 + 23.89 + 24.15 + 23.16 + 24.45 + 24.15 + 24.69$$

$$c = 238.57$$

$$d := 23.40 + 23.96 + 24.13 + 23.75 + 24.74 + 22.53 + 25.45 + 24.85$$

$$d = 192.81$$

$$\text{GTave} := \frac{c + d}{18}$$

$$\text{Average G/T on T1-VSAT} \quad \text{GTave} = 23.966$$

10.80 dB @ 10^{-6} BER, Theory

Modem Implementation Loss Uplink = 3.0 dB

Downlink = 2.0 dB

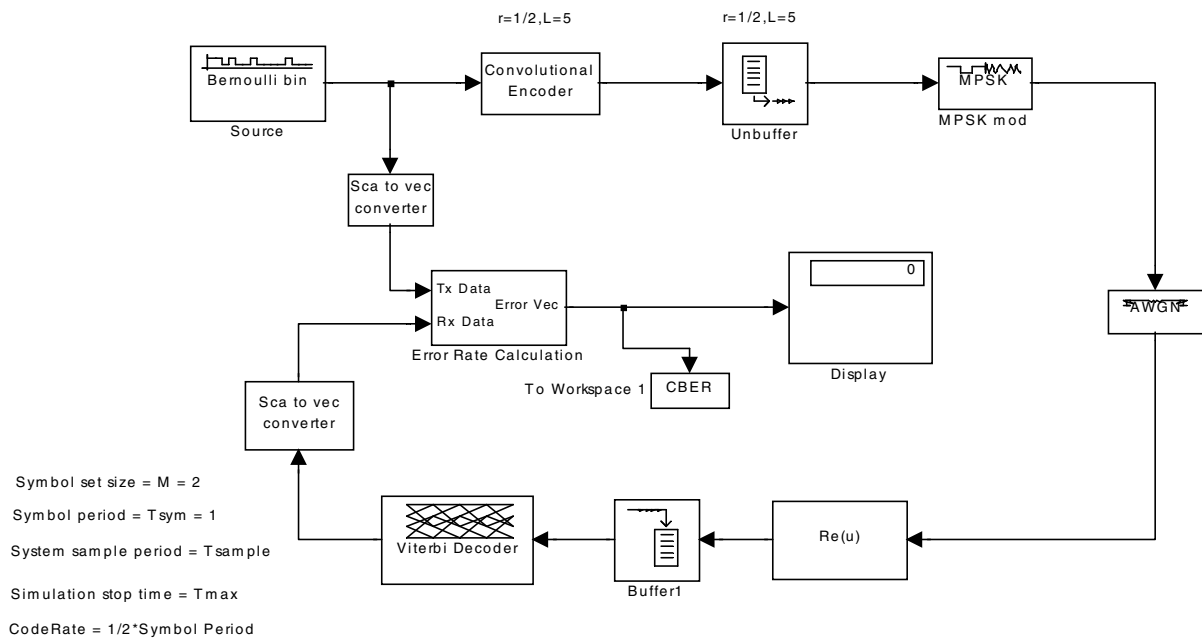
Digital Satellite Communication Link Calculation Result Summary

Uplink C/No	$CNO_{up} = 92.234$	dBW-Hz
Downlink C/No	$CNO_{dw} = 102.08$	dBW-Hz
Overall C/NO	$CNO = 91.806$	dBW-Hz
Downlink Eb/No	$EbNO_{dw} = 18.666$	dB
Downlink Margin	$DW_{marg} = 7.866$	dB
Uplink Eb/No	$EbNO_{up} = 14.341$	dB
Uplink Margin	$Up_{marg} = 3.541$	dB

APPENDIX 2

SIMULINK MODEL OF CONVOLUTIONAL CODING

One Channel BPSK Convolutional Coded Block Diagram



APPENDIX 3

MATLAB CODE FOR GENERATING BER TIME ENHANCEMENT FACTOR FOR ACTS PROPAGATION TERMINAL DATA

```
% This code will convert a given fade CDF and coded and uncoded
% system curve to a BER enhancement factor curve.

% Input:
%   Fade CDF
%   Format: Fade(dB) (as positive number)   Availability (%)
%   Coded System Curve
%   Format: Eb/No   Coded BER
%   Uncoded System Curve
%   Format: Eb/N0 Uncoded BER

clear all
% If polyn = 1, create uncoded data from file
% If polyn = 0, use equation to create uncoded data

polyn = 1;

% EbNoVecL is the Eb/N0 values that are extrapolated beyond the
% measured Eb/N0 values using the polynomial

EbNoVecL=[0:1:20];

% Read in fade CDF for all 7 sites and coded system curve
% FadeData is a 2 column vector - the 1st column is the fade, the
% second column is availability

fid = fopen ('APTcdf.txt');
line = fgetl(fid); % First 2 lines are not needed
line = fgetl(fid);
[FadeData count] = fscanf (fid, '%f %f ...
                          %f %f %f %f', [15 inf]);
FadeData = FadeData';
fclose(fid);

% Read coded system curve
% CodedData is a 2 column vector - the 1st column is Eb/N0 and the
% second column is BER

fid = fopen ('CodedSystem.txt');[CodedData count] = fscanf(fid, ...
                  '%f %e', [2 inf]);
CodedData = CodedData';
fclose(fid);

% If polyn = 1, read in uncoded system curve
```

```

% UncodedData is a 2 column vector - the 1st column is Eb/N0 and the
% second column is BER

if polyn == 1
    fid = fopen ('UncodedSystem.txt');
    [UncodedData count] = fscanf(fid,'%f %e',[2 inf]);
    UncodedData = UncodedData';
    fclose(fid);
else
    BERtheory = 0.5*(1-erf(sqrt(10.^(EbNoVecL(:)-1.5)/10)));
end

% Create polynomial for coded system curve

pc = polyfit(CodedData(:,1),log10(CodedData(:,2)),4);
popc = 10.^polyval(pc,EbNoVecL(:));
ptc = polyfit(EbNoVecL(:),log10(popc),4);

% Create polynomial for uncoded system curve is polyn = 1

if polyn == 1
    pu = polyfit(UncodedData(:,1),log10(UncodedData(:,2)),4);
    popu = 10.^polyval(pu,EbNoVecL(:));
    ptu = polyfit(EbNoVecL(:),log10(popu),4);
end

% Plot two system curves
figure(1)
semilogy(CodedData(:,1),CodedData(:,2),'rs-',
    UncodedData(:,1),UncodedData(:,2),'bd-');
axis([0 10 10^-7 10^0]);
grid on;
XLABEL('Eb/N0 (dB)');
YLABEL('Bit Error Rate Probability');
TITLE('One Channel BPSK Convolutional Coding Performance');
legend('Convolutional coded','Non coded');

% Plot results using polynomials
figure (2)
semilogy(UncodedData(:,1),UncodedData(:,2),'--mo',EbNoVecL(:),popu,...
    '-.r*',CodedData(:,1),CodedData(:,2),'-xg',EbNoVecL(:),popc,':dc')
axis([0 20 10^-35 10^4]);
XLABEL('Eb/No (dB)');
YLABEL('Bit Error Rate Probability');
TITLE('Curve fitting for BER vs. EbNo');
legend ('Uncoded BER curve','Uncoded BER polynomial','Original ...
    Coded BER curve','Coded BER Polynomial')
grid on

% Must convert fade to Eb/N0
% Assumes 0 fade is equal to Eb/N0 of 15.3 dB

EbN0 = 15.3 - FadeData(:,1)
NumPosFade = 0;

```

```

[RowFade ColFade] = size(FadeData);
for n=1:1:RowFade
    if EbN0(n) >= 0
        CBERforFade(n) = 10^polyval(ptc,EbN0(n));
        if polyn == 1
            UBERforFade(n) = 10^polyval(ptu,EbN0(n));
        else
            UBERforFade(n) = 0.5*(1-erf(sqrt(10^(EbN0(n)-1.5)/10)));
        end
        NumPosFade = NumPosFade + 1;
    end
end

% Subtract the availabilities to determine BER enhancement factor

for BinNo = 2:1:8
    BERSpecVal(BinNo-1) = 10^-(BinNo)
end;

% Cycle through each of the 7 APT locations
for FadeLoc=1:1:7
    FadeCol = FadeLoc*2
    % Find coded and uncoded BER availability for the given range of
    % Fade CDF values
    Spec_P_UDBER(FadeLoc,:) = ...
        interp1 (UBERforFade,FadeData(1:NumPosFade,FadeCol),...
            BERSpecVal,'linear')
    Spec_P_CDBER(FadeLoc,:) = ...
        interp1 (CBERforFade,FadeData(1:NumPosFade,FadeCol),...
            BERSpecVal,'linear')
    BERenhFactor(FadeLoc,:)=Spec_P_UDBER(FadeLoc,:) ...
        - Spec_P_CDBER(FadeLoc,:)
end

% Plot Fade availability curve
figure(3)
semilogy(FadeData(:,1),FadeData(:,2),'r+-
',FadeData(:,1),FadeData(:,4),'mo-')
hold on
semilogy(FadeData(:,1),FadeData(:,6),'gd:',FadeData(:,1),...
    FadeData(:,8),'r*:')
semilogy(FadeData(:,1),FadeData(:,10),'gx-', ...
    FadeData(:,1),FadeData(:,12),'bs-', ...
    FadeData(:,1),FadeData(:,14),'cd:')
xlabel('Fade (dB)')
ylabel('% Time Exceeded')
title('Fade CDF')

legend('Florida','Alaska','Vancouver','Colorado','Maryland',...
    'Oklahoma','New Mexico')
grid on
axis([0,30,1e-3,100])
%print -dmeta EbNOCDF
hold off

```

```

% Plot BER availability curve
figure (4)
loglog(UBERforFade(:), FadeData(1:NumPosFade,2), 'r+-', ...
       CBERforFade(:), FadeData(1:NumPosFade,2), 'r+:')
xlabel('BER')
ylabel('% Time Exceeded')
title('BER CDF - Florida')
legend('Uncoded BER CDF', 'Coded BER CDF')
grid on
axis([1e-9,1,10e-4,100])

% Plot BER enhancement Factor curve
figure (5)
semilogx (BERSpecVal, BERenhFactor(1,:), 'r+-', ...
          BERSpecVal, BERenhFactor(2,:), 'mo-')
hold on
semilogx (BERSpecVal, BERenhFactor(3,:), 'gd:', ...
          BERSpecVal, BERenhFactor(4,:), 'r*:')
semilogx (BERSpecVal, BERenhFactor(5,:), 'gx-', ...
          BERSpecVal, BERenhFactor(6,:), 'bs-')
semilogx (BERSpecVal, BERenhFactor(7,:), 'cd:')
hold off
xlabel('BER Level')
ylabel ('Percent of Time Increased (%)')
title ('BER Enhancement Factor')
legend('Florida', 'Alaska', 'Vancouver', 'Colorado', 'Maryland', ...
       'Oklahoma', 'New Mexico')
grid on
axis([1e-8,1e-2,0,2])

% Plot Eb/N0 availability curve
figure (6)
semilogy(EbN0, FadeData(:,2), 'r+-', EbN0, FadeData(:,4), 'mo-')
hold on
semilogy(EbN0, FadeData(:,6), 'gd:', EbN0, FadeData(:,8), 'r*:')
semilogy(EbN0, FadeData(:,10), 'gx-', EbN0, FadeData(:,12), 'bs-', ...
         EbN0, FadeData(:,14), 'cd:')
xlabel('EbN0 (dB)')
ylabel('% Time Exceeded')
title('EbN0 CDF')
legend('Florida', 'Alaska', 'Vancouver', 'Colorado', 'Maryland', ...
       'Oklahoma', 'New Mexico')
grid on
axis([0,30,1e-3,100])
hold off

```

INDEX OF SYMBOLS

ACTS	Advanced Communication Technology Satellite
APT	ACTS Propagation Terminal
BBP	Baseband Processor
BER	Bit Error Rate
BPSK	Binary Phase Shift Keying
CDF	Cumulative Distribution Function
E_b/N_0	Bit Energy to Noise Ratio
FEU	Feed Electronic Unit
ITU – R	International Telecommunications Union – Radiocommunication
IBOW	Inbound Orderwire
Ka-band	30/20 GHz
LNC	Low Noise Converter
Mbps	Mega Bits Per Second
MCS	Master Control Station
MPTS	Modem Processor Test Set
MspS	Mega Symbols Per Second
MSM	Microwave Switch Matrix
NGS	NASA Ground Station
NASA	National Aeronautic and Space Administration

SNR	Signal to Noise Ratio
TDMA	Time Division Multiple Access
TIE	Terrestrial Interface Equipment
VSAT	Very Small Aperture Terminal

REPORT DOCUMENTATION PAGE

Form Approved
OMB No. 0704-0188

Public reporting burden for this collection of information is estimated to average 1 hour per response, including the time for reviewing instructions, searching existing data sources, gathering and maintaining the data needed, and completing and reviewing the collection of information. Send comments regarding this burden estimate or any other aspect of this collection of information, including suggestions for reducing this burden, to Washington Headquarters Services, Directorate for Information Operations and Reports, 1215 Jefferson Davis Highway, Suite 1204, Arlington, VA 22202-4302, and to the Office of Management and Budget, Paperwork Reduction Project (0704-0188), Washington, DC 20503.

1. AGENCY USE ONLY (<i>Leave blank</i>)	2. REPORT DATE July 2001	3. REPORT TYPE AND DATES COVERED Technical Memorandum	
4. TITLE AND SUBTITLE Analysis of Fade Detection and Compensation Experimental Results in a Ka-Band Satellite System		5. FUNDING NUMBERS WU-322-10-2A-00	
6. AUTHOR(S) Sandra Johnson			
7. PERFORMING ORGANIZATION NAME(S) AND ADDRESS(ES) National Aeronautics and Space Administration John H. Glenn Research Center at Lewis Field Cleveland, Ohio 44135-3191		8. PERFORMING ORGANIZATION REPORT NUMBER E-12838	
9. SPONSORING/MONITORING AGENCY NAME(S) AND ADDRESS(ES) National Aeronautics and Space Administration Washington, DC 20546-0001		10. SPONSORING/MONITORING AGENCY REPORT NUMBER NASA TM-2001-210984	
11. SUPPLEMENTARY NOTES This report was submitted as a thesis in partial fulfillment of the requirements for the degree Master of Science in Electrical Engineering to the University of Akron, Akron, Ohio, May 2000. Responsible person, Sandra Johnson, organization code 6130, 216-433-8016.			
12a. DISTRIBUTION/AVAILABILITY STATEMENT Unclassified - Unlimited Subject Category: 17 Available electronically at http://gltrs.grc.nasa.gov/GLTRS This publication is available from the NASA Center for AeroSpace Information, 301-621-0390.		12b. DISTRIBUTION CODE	
13. ABSTRACT (<i>Maximum 200 words</i>) The frequency bands being used for new satellite communication systems are constantly increasing to accommodate the requirements for additional capacity. At these higher frequencies, propagation impairments that did not significantly affect the signal at lower frequencies begin to have considerable impact. In Ka-band, the next logical commercial frequency band to be used for satellite communication, attenuation of the signal due to rain is a primary concern. An experimental satellite built by NASA, the Advanced Communication Technology Satellite (ACTS), launched in September 1993, is the first U.S. communication satellite operating in the Ka-band. In addition to higher carrier frequencies, a number of other new technologies, including onboard baseband processing, multiple beam antennas, and rain fade detection and compensation techniques, were designed into the ACTS. Verification experiments have been conducted since the launch to characterize the new technologies. The focus of this thesis is to describe and validate the method used by the ACTS Very Small Aperture Terminal (VSAT) ground stations in detecting the presence of fade in the communication signal and to adaptively compensate for it by the addition of burst rate reduction and forward error correction. Measured data obtained from the ACTS program is used to validate the compensation technique. In this thesis, models in MATLAB are developed to statistically characterize the increased availability achieved by the compensation techniques in terms of the bit error rate time enhancement factor. Several improvements to the ACTS technique are discussed and possible implementations for future Ka-band systems are also presented.			
14. SUBJECT TERMS ACTS; Ka-band; 30/20 GHz; Satellite communications; Technology verification; Propagation; Fade mitigation		15. NUMBER OF PAGES 94	
		16. PRICE CODE	
17. SECURITY CLASSIFICATION OF REPORT Unclassified	18. SECURITY CLASSIFICATION OF THIS PAGE Unclassified	19. SECURITY CLASSIFICATION OF ABSTRACT Unclassified	20. LIMITATION OF ABSTRACT